Escola de Camins
Escola Tècnica Superior d'Enginyeria de Camins, Canals i Ports
UPC BARCELONATECH

PROJECTE O TESINA D'ESPECIALITAT

Títol

Moment redistribution in continuous steel-concrete composite beams.

Autor/a

Isaac Francisco Gimeno Sanz

Tutor/a

Enrique Mirambell Arrizabalaga

Departament

Enginyeria de la Construcció.

Intensificació

Anàlisi i projectes d'Estructures.

Data

Juliol 2013

Moment redistribution in continuous steel concrete composite beams.

Summary

This paper presents a research carried out on continuous steel-concrete composite beams. The research focuses on the flexural behaviour of continuous composite beams, laterally restrained, at short term. Hence, the analysis is centered on Ultimate Limit State (ULS). Numerical finite element models are developed with ADAPTIC (Izzudin 1991) in order to calculate the ultimate capacity of the beams. This capacity is considered to be limited by the local buckling of structural steel and/or the maximum elongation of reinforcing bars. The accuracy of the models' predictions is evaluated comparing the results obtained against previous experimental outcomes. Nonlinear behaviour of the component materials, steel, concrete, reinforcing steel and shear connection, is taken into account. The numerical results are then used to calculate the permissible moment redistribution that satisfies the ULS requirements. An extensive parametric study is carried out to determine the influence of the main geometrical and mechanical parameters governing the composite beams response at ULS. Different classes for composite sections (Eurocode 4, CEN 2004b, Eurocode 3, CEN 2005) as well as different grades for structural steel and different characteristic compressive strengths for concrete are considered. The results obtained are discussed and compared with the moment redistribution limits provided by current codes of practice (Eurocode 4, CEN 2004b, AISC 360-05, AISC 2005). At the expenses of the results obtained, it seems that the limits stated by these codes are unconservative for some types of beams, under specific circumstances.

Redistribución de momento flector en vigas continuas mixtas de acero y hormigón.

Resumen

El presente documento muestra la investigación llevada a cabo en el campo de las vigas mixtas de acero y hormigón. La investigación se centra en el comportamiento a flexión de vigas mixtas continuas, con el movimiento lateral impedido y a corto plazo. Por lo tanto, el análisis se centra en el Estado Límite Último (ELU). Se ha desarrollado un modelo numérico de elementos finitos usando un software llamado ADAPTIC (Izzudin 1991) para calcular la capacidad última de las vigas. Dicha capacidad está limitada tanto por el pandeo local del acero estructural como por la máxima deformación en el acero de refuerzo. La precisión del modelo se valida comparando los resultados obtenidos por el modelo frente a los obtenidos por estudios experimentales. Se considera comportamiento no lineal de todos los materiales que componen la viga: acero estructural, hormigón, acero de refuerzo y sistema de conexión. Los resultados numéricos serán utilizados con el objetivo de calcular la redistribución de momento flector disponible que satisface los criterios de ELU. También se lleva a cabo un extenso estudio paramétrico para determinar la influencia de los principales parámetros mecánicos y geométricos que gobiernan la respuesta de las vigas mixtas bajo ELU. Se consideran diferentes clases así como diferentes grados de secciones de acero estructural (Eurocode 4, CEN 2004b, Eurocode 3, CEN 2005) y diferentes resistencias características a compresión para el hormigón. Los resultados obtenidos se juzgan y comparan con los límites de redistribución de momento flector propuestos por diferentes códigos internacionales (Eurocode 4, CEN 2004b, AISC 360-05, AISC 2005). A expensas de los resultados obtenidos, parece ser que dichos límites son poco conservativos para algunas vigas y bajo ciertas circunstancias.

Acknowledgements.

- I would like to express my thankfulness to Dr. Lorenzo Macorini for all his remarks and advice that helped me during this project.

- I would also like to thank to the postgraduates students, Francisco Brás and Corrado Chisari, for all the time they dedicated to me, providing guidance, advice and instructions with Adaptic and Linux. Without them, the completion of this project would not have been possible.

- I would like to thank the piece of advice received from Dr. Enrique Mirambell, who, as my supervisor at Universitat Politècnica de Catalunya, helped me when I needed.

- Finally, for their warm welcome and their help and support given along this project, I would like to express my sincere gratitude to all the Civil and Environmental Engineering Department from Imperial College.

Barcelona, July 2013.

Table of contents.

1. Introduction.

1.1 General concepts about steel-concrete composite structures.

A steel-concrete composite structure is a system which couples the concrete and steel materials in order to make them work together against the loading that the structure has to resist. This system is widely used for both, buildings and short and medium span bridges. However, there are other systems such as encased I-sections used in steel frames with several benefits too.

The world of composite structures has grown its market during the lasts decades across several countries from Europe, USA, Canada and Australia. The different systems are efficient and attractive to designers due to its economical, structural and construction benefits. The firsts lie on the fact of the reduction in steel weight while introducing a different material (concrete) which is cheaper than steel. The structural advantages consist on a strengthening and stiffening of the structure when adding a top flange made of concrete in either composite beams or bridges. The consequence of that is that the Serviceability Limit States (SLS) are not usually the decisive factor when designing because the system reduces considerably both, the vibrations and the vertical displacements. Moreover, when talking about columns and frames, the benefits of encasing the steel section within the concrete are also relevant. Not only does the concrete protect the steel section from the fire, but it also reduces the effective slenderness of the column, and so increases its buckling load. Finally, the quick construction and a reduction in floor depths, which allows a better integration of the services, have an impact on the economy of the construction too.

Therefore, to sum up, composite construction is competitive when dealing with medium-long spans in buildings, short-medium spans in bridges and where rapid construction or low-medium level of fire protection is needed.

1.2 Concepts about steel and concrete composite beams.

A composite beam consists of a steel member in the bottom part and a concrete flange at the top part. The steel member is usually an I-shaped rolled or welded beam whereas the concrete flange is usually part of a concrete slab. The width of this top concrete flange is defined in the codes as an effective width which is the minimum of the distance between the centres of two consecutive beams, and a width defined by experimental formulas established in those codes. It depends on the region that we are analysing the beam, whether it is sagging moment region (with tensile stresses at the bottom) or hogging moment region (with tensile stresses at the top).

The concrete and the steel parts are linked thanks to a connection system made of headed studs. These are usually welded to the top flange of the steel member and fully embedded into the concrete slab. The connection system generally allows a relative slip between the bottom fibre of concrete and the top flange of steel section. Therefore, the connection system has to be regarded as flexible. The concrete, the structural steel, and reinforcing steel will be characterized by nonlinear behaviours.

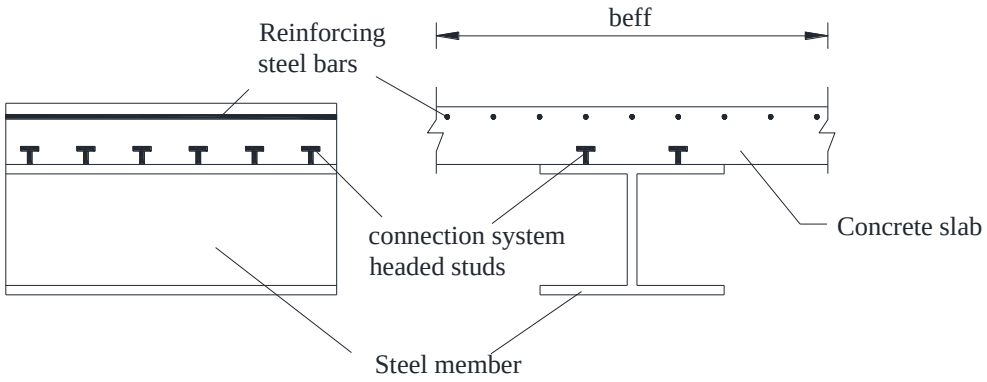

Figure 1.1. Parts of a steel and concrete composite beam.

The mechanical properties of the component materials are best exploited at simply supported beams since the concrete remains in compression and steel in tension along the whole beam. However, these types of beams can also be used for continuous beams. It must be taken into account that, having the same cross section along the whole beam due to construction reasons, next to the inner supports, the continuous beam is under hogging bending moment, which implies that the concrete is under tensile stresses and part of the bottom section under compression. Tensile stresses in the concrete slab may cause cracking development within the concrete and excessive elongation of the reinforcing bars, whereas compressive stresses along the web and the bottom flange of the steel member can lead to local buckling. Therefore, in those areas, the resistance of the section is lower because the mechanical properties of the materials are not exploited properly. Moreover, the elastic bending moment envelope shows that the moment around those interior supports is higher than along the rest of the beam (in absolute value). Accordingly with that, the beam becomes much weaker around the inner supports than in sagging bending moment regions. Therefore, is at that stage when, as it will be explained later, the redistribution of the bending moment diagram becomes crucial to avoid the temptation to design beams to resist sagging bending moment and expand the resultant cross section along the beam, leading to an expensive and non-efficient design.

Finally, the research is centred on beams that are laterally restrained. In sagging moment regions the bottom flange is under tension whereas the top flange is, in many cases, under compression. However, as the Eurocode 4(CEN 2004b) states, if the shear connection is designed in accordance to its clause 6.6, all flanges attached to a solid concrete slab can be assumed to be laterally stable, provided that lateral instability of concrete slab is prevented. Therefore, in sagging moment regions, it can be considered that is unlikely that any of both flanges experience lateral buckling. Despite that, possible local buckling at the web has to be taken into account. On the other hand, in hogging moment regions, the flange under compression stresses is the bottom one, and this one has no effective attachment to any part of the composite beam. Consequently, this fact can lead to the lateral buckling of the whole beam. However, laterally restraints can be provided in order to avoid that the lateral local buckling could be the restrictive condition. There are different systems to restrain laterally the bottom flange such as x-bracings between parallel beams, displacing bearing stiffeners on each side of the web… However, the one that most designers propose is the one showed in the following picture:

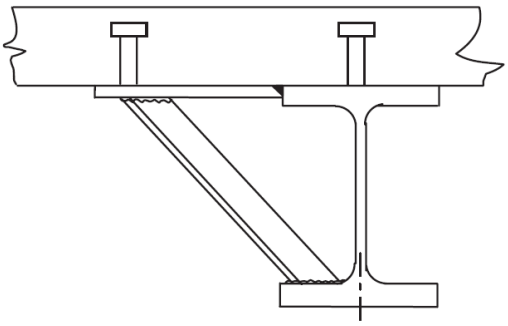

Figure 1.2. Lateral restraint to bottom flange in hogging moment regions for solid slabs. (Hendy and Johnson, 2006).

1.3 Objectives.

The main objectives of the present research are the ones enumerated below:

- ✓ Review of literature related to the analytical, experimental and numerical investigation of composite structures, and in particular, to those that refers to composite beams with solid slabs. In addition, the literature related with the collapse of steel sections (in local buckling conditions) will be needed to be revised, too.

- ✓ Study of the current European code Eurocode 4 (CEN 2004b) relative to the design of steel and concrete composite structures for buildings. Furthermore, some aspects from other codes as Eurocode 2 (CEN 2004.a) and Eurocode 3 (CEN 2005) will have to be taken into account.

- ✓ Study and development of a numerical model which allows representing the structural response of concrete and steel composite beams under incremental loading. The model must reproduce the nonlinearity of the mechanical properties of the materials as well as the flexibility of the connection system. This model will be implemented with a software called ADAPTIC developed at Imperial College of London (Izzuddin 1991).

- ✓ Validate the developed numerical model with previous experimental tests carried out in both, laboratories or in situ. Compare the model with other numerical models developed before. That is needed in order to ensure that the model will represent the beams that we want to study in an acceptable way.

- ✓ Study and compute the permissible moment redistribution in propped cantilevers and fixed ended beams for different cross section classes (class 1 and 2) Eurocode 3 (CEN 2005). This percentage of redistribution must be calculated from two different situations of collapse:

    - Collapse due to formation of mechanism.
    - Collapse due to ultimate rotation attainment.

- ✓ Develop a parametric study with a great deal of different beams in order to find a moment redistribution domain that satisfies the rotation compatibility at interior supports of continuous beams.

- ✓ Identify the mechanical or geometrical parameters which have significant influence on the permissible moment redistribution and study how they influence the allowable moment redistribution of the composite beams.

- ✓ Compare the limits for the redistribution of the obtained domain with the recommendations given in the Eurocode 4 (CEN 2004b). Moreover, the American code AISC 360-05 (AISC 2005) will be also taken into account when analysing the limits for the moment redistribution. Conclude whether these limits are on the safe side or not.

1.4 Research scope.

The research is focused on continuous steel-concrete composite beams, being the concrete flange part of a concrete solid slab. The general features of the model are described below:

- ✓ Short term analyses were carried out. Therefore, only Ultimate Limit States (ULS) are taken into account. Serviceability Limit States (SLS) remain out of this research's scope.

- ✓ The steel sections will be those that belong to UKB steel sections which features are detailed in the booklet *Advance® sections* of Corus Construction & Industrial.

- ✓ The allowable moment redistribution of composite beams with steel cross sections of class 1 and 2 Eurocode 3 (CEN 2005) was computed.

- ✓ Structural steel of different grades is also taken into account (235, 275 and 375 N/mm^2).

- ✓ Different concrete's characteristic compressive strengths (30 and 40 N/mm^2) are considered.

- ✓ The influence of different degrees of shear connection will be also investigated.

- ✓ Low ductility reinforcing steel bars are contemplated [$\varepsilon ru \geq 2.5\%$, class A according to Comite Euro-International du Beton (CEB) 1993] with S430 grade.

- ✓ The influence of higher ductility steel reinforcement grades will be also studied.

- ✓ The research uniquely involves solid slabs.

- ✓ The inner spans of the continuous beams are idealised as fixed ended beams while the outer spans are represented by propped cantilevers. Both of them are subjected to uniformly distributed load (UDL).

- ✓ 19mm headed studs are modelled. The possible uplift will be neglected. As shown in experimental studies carried out by Johnson and Molenstra (1991), this is a good approach. Moreover, that is confirmed in the validation of the model with some experimental tests.

1.5 Contents and structure of the report.

The present thesis introduces the study of the flexural behaviour of continuous steel concrete composite beams. The main purpose is to evaluate the allowable bending moment redistribution of those beams when they are used mainly in buildings and short-span or medium-span bridges.

Along the **2nd chapter** from the present document the reader will find out about the development of a nonlinear numerical model to simulate the behaviour of both, propped cantilevers and fixed end beams, when the load is increased up to the attainment of rotation capacity at the fixed supports of the mentioned beams. Firstly, a description of the finite element used will be showed. Secondly, the reader will find the following:

i. Brief description of the constitutive laws used.
ii. Validation of the model against experimental results.
iii. Detailed description of the numerical analysis of a continuous composite beam.

After that, in the **3rd chapter** the method to compute the allowable moment redistribution is described. First of all, the particular cases for Class-1 and Class-2 cross sections are explained. Following that, the reader will find how to calculate the redistribution due to two different causes of collapse:

i. Due to rotation capacity attainment at fixed supports.
ii. Due to the development of a plastic mechanism.

Within the **4th chapter** the parametric study is exposed. It is described all the parameters against which the allowable redistribution is evaluated. Furthermore, all the geometrical and mechanical parameters, and their different values taken into account, are exposed. All the steel UKB standard sections taken into consideration are described. Finally, a criterion to avoid analysing beams that are out of the technical interest is also showed.

The outcomes are showed in the **5th chapter**. The results are showed for class-1 steel cross sections, and afterwards, for class-2 steel cross sections. For both cases, the way in which the results are presented is as follows:

i. Full shear connection.
ii. Partial shear connection with a degree of connection of 0.75.
iii. Partial shear connection with a degree of connection of 0.5.

After that, the influence of some parameters is analysed:

i. Type of loading
ii. Ductility grade of reinforcing steel.

iii. Degree of connection.
iv. Non-dimensional parameters from the parametric study.
v. Local buckling criteria.

Finally, a domain of permissible redistribution is suggested.

The **6th chapter** expose the conclusions obtained from this research before pointing out the **references** consulted.

Finally, within the **appendix** the reader will find a piece of the overall numerical results with which he will be able to check the statements done along the report in what the outcomes is concerned. They are focus on one type of steel cross section and only for class1 because the results show the same behaviour for the rest of beams and for class 2 steel cross sections. For each case, an overall of 81 beams' results are shown due to this is the half of the number obtained when combining all the parameters discussed on section 4.

2. Nonlinear numerical model.

The whole finite element, shown in Figure 2.1, consists of two Navier-Bernoulli's beams which represents the concrete slab and the steel member, respectively. The centers of mass of both beams are linked by a system of nonlinear springs which represent the connection system. At the beginning of the analysis, both centers are coincident in the horizontal coordinate. As the beam starts to deform, the horizontal and vertical slips start to take place at the contact surface between both materials. However, neglecting the uplift leads to a good approach in accordance with experimental studies carried out by Johnson and Molenstra (1991). Perfect bond between the reinforcement and the concrete is assumed. The whole beam is divided in several finite elements, while the concrete slab and the steel profile are divided in 50 layers to account the variation of stress along both profiles.

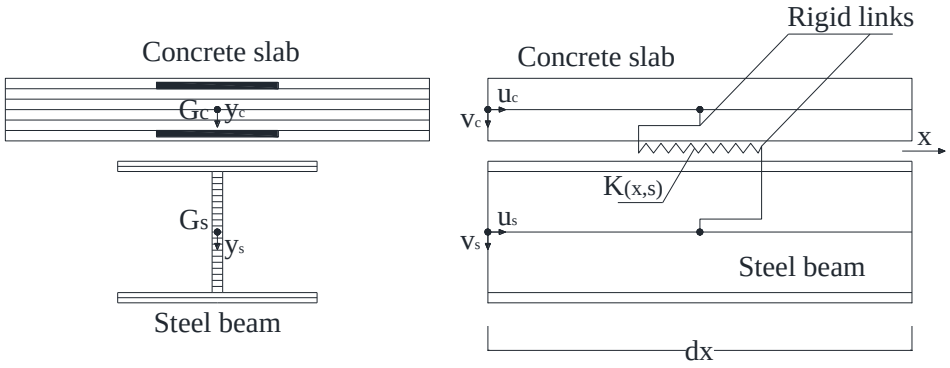

Figure 2.1: Finite-element model.

2.1 Constitutive relationships.

The constitutive relationships have been chosen in accordance to the availability of the models of the software used. All of them are explained in detail below.

2.1.1 Constitutive relationship for steel.

For both, steel profile and reinforcing bars, a bilinear elasto-plastic law with strain hardening, shown in Figure 2.2, is adopted, where ε_{ru} is the ultimate uniform tensile strain for reinforcing steel. A 1% of kinematic strain hardening (μ) will be assumed (Figure 2.2). The difference between both will be the yield stress (fry), while Young's Modulus (E) will remain constant for both steels. The model chosen from ADAPTIC will be *stl1*.

2.1.2 Constitutive relationship for concrete.

For concrete in compression a nonlinear law will be proposed (Mander et. Al, 1988). The model shown in Figure 2.3, called *con2* in ADAPTIC, will be used for this purpose, where f_c is the compressive strength, f_t the tensile strength and the ε_{co} the crushing strain. It models

concrete in tension with elastic behaviour only. For concrete in compression, the linear elastic behaviour is followed by elastic-plastic behaviour with a softening final path. A constant confinement is assumed with this model. The model takes into account the confinement factor, which is supposed to be equal 1 in the present research.

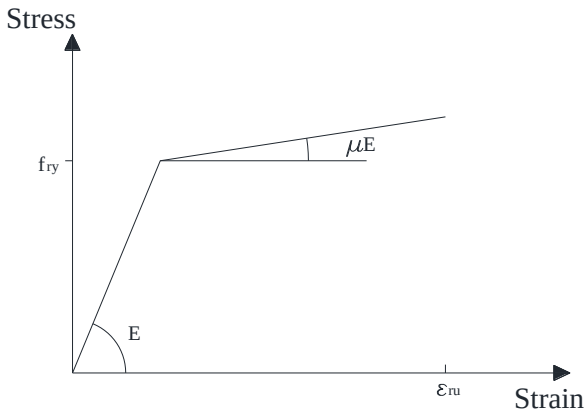

Figure 2.2: Constitutive relationship for steel.

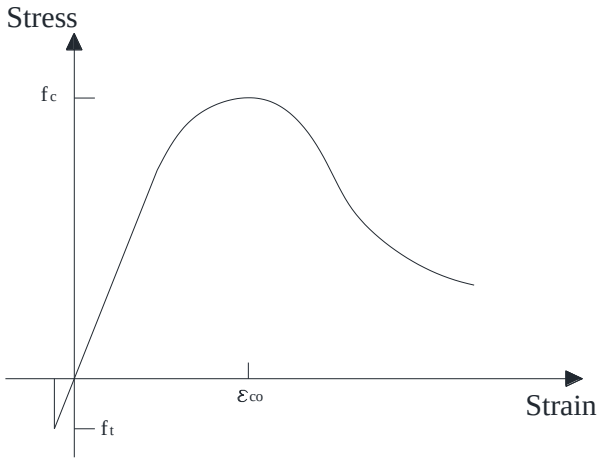

Figure 2.3: Constitutive relationship for concrete.

2.1.3 Constitutive relationship for connectors.

Exponential load-slip relationship will be assumed for the connection system (Figure 2.4):

$$P = P_d\left(1 - e^{-\beta.s}\right)^{\alpha} \quad (1)$$

Where P_d is the design value for stud's shear strength and s is the slip in mm. Besides, β and α are coefficients which will be obtained from recent experimental studies (Johnson and Molenstra, 1991) despite the equation was obtained by earlier research (Ollgaard et. al 1971). Since this model is not available with the software that we are going to use, we will model the connectors as nodal springs with a tri-linear approach to the load mentioned before as shown in Figure 2.5.

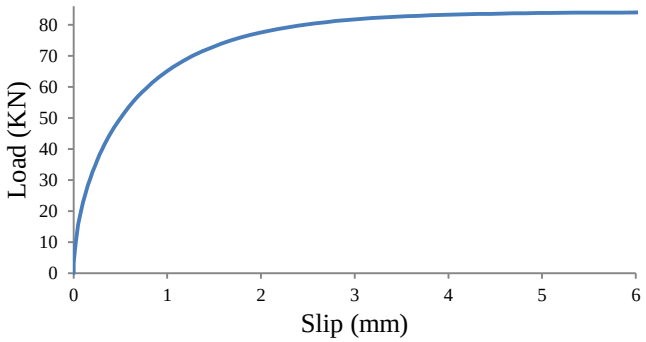

Figure 2.4: Exponential load-slip relationship for shear connection system.

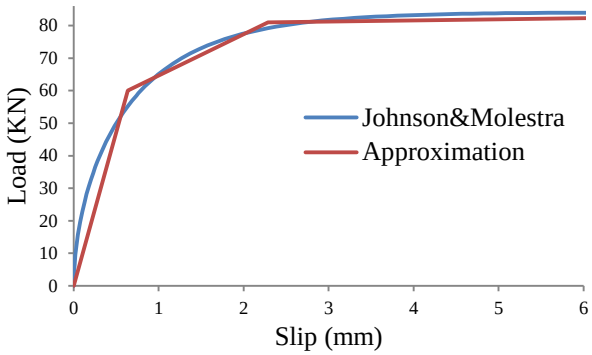

Figure 2.5: Approximation of the exponential load-slip relationship to a trilinear model.

Therefore, *jel2* point links will be used to represent the shear studs with *smrt* curve to take into account the stiffness variation during the load increasing (trilinear symmetric elasto-plastic curve type).

It must be pointed out that, as shown in Figure 2.5, the vertexes of the approximated tri-linear shape are not coincident with the actual model curve. Further discussion on this issue will be exposed at the end of next section.

2.2 Validation of the model.

Table 2.1: Features of the Teraskiewicz's beam.

I-Section Steel Beam.		**Shear Connectors**		**Concrete**		**Reinforcement**	
Young's modulus (N/mm^2)	200000	Diameter (mm)	9	Young Modulus (N/mm^2)	27600	Young's modulus (N/mm^2)	200000
Strain Hardening	0.5%	Length (mm)	50	Poisson's Ratio	0.15	Yield Stress (N/mm^2)	310
Yield Stress (N/mm^2)	285	Spacing (mm)	146	f_{ck} (N/mm^2)	48	Top & Bottom reinforcement diameter (mm)	8
Flange thickness (mm)	9.6	Paired (mm)				Top spacing (mm)	65
Web thickness (mm)	5.9					Bottom spacing (mm)	204

The numerical model has been validated with the experimental research carried out by Teraskiewicz (1969). It consisted on testing 6.7m long, two-span continuous composite beam with point loading at mid span. The depth of the steel member was 152mm, whereas the depth of the concrete slab was 60.3mm and its width was 610mm. A propped cantilever idealizing

the right span of the two-span beam was modeled. The numerical model was designed in order to make the point loading coincident with a node of the mesh. The shear connection was also idealized as nonlinear behaviour springs. The headed studs used by Teraskiewicz (1969) were modeled properly by the force-slip relationship proposed by Yam and Chapman (1972):

$$Q = 32(1 - e^{-4.75xS}) \quad (2)$$

where Q is the shear force in kilonewtons and S is the slip in millimeters. This curve was idealized as a symmetric trilinear behaviour, as explained in 2.1.3. The details of the beams are shown in Table 2.1.

Figs. 2.6, 2.7 and 2.8 compare the results predicted by the numerical model with the results measured by the experiments at a load of 122kN, which is 91% of the predicted ultimate loading. The agreement in the mentioned figures shows the reliability of the model. The proposed model fits well the experimental results in terms of vertical displacement. Regarding local parameters such as the slip and the strain at the lower fiber of the steel member, the model has an acceptable behaviour, too. Concerning the fact of neglecting the uplift, we can conclude that it is a good approach. As shown in all comparisons, but more specifically, in the slip comparison, it does not lead to a significant difference. Therefore, this simplified hypothesis may lead to sufficiently accurate results even for composite beams that are loaded near the collapse (ULS).

As shown in Figure 2.8, the plastic hinges are developed around the inner support and the mid-span. Within these areas take place great strains at the bottom of the steel member. In the inner support the compression strain may lead to local buckling and will be one of the limits of the cross section rotation capacity.

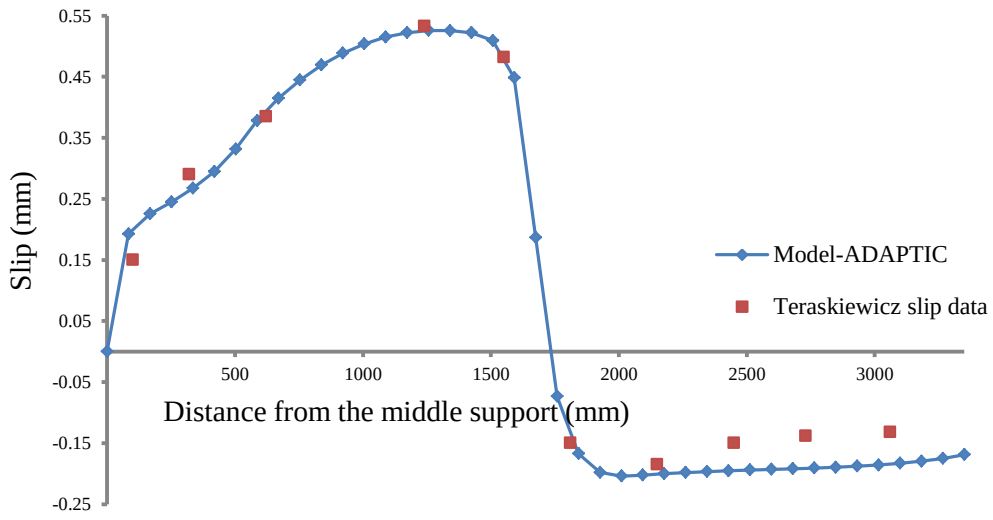

Figure 2.6: Slip distribution.

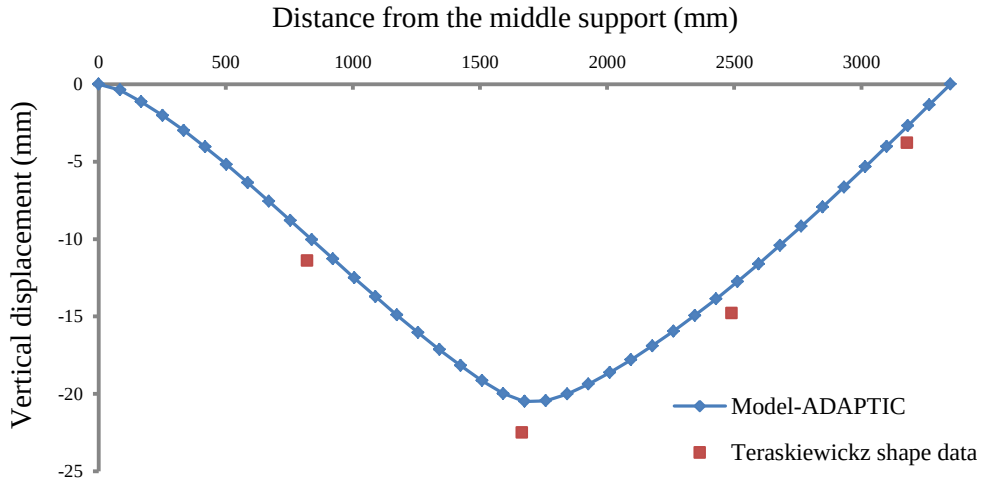

Figure 2.7: Deflected shape.

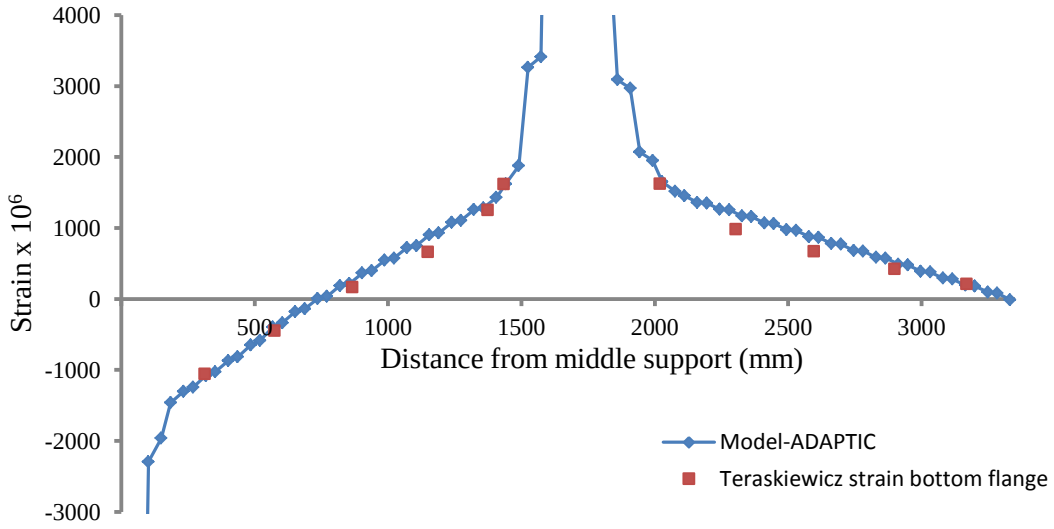

Figure 2.8: Strains on bottom steel flange.

Regarding the issue of the tri-linear approximation for the load-slip curves of the headed-studs, it must be observed at Figure 2.6 that the slips around pinned supports are quite small, but non negligible. Therefore, at the ultimate load, the studs within this area have a load-slip relationship that belongs to the first path of the tri-linear model. At this stage, the exponential curve defined by Johnson and Molestra (1991) (Figure 2.5) have a large tangent stiffness that drops down dramatically along the two following paths.

The models that were carried out with the vertexes being coincident with the actual curve worked with a much lower stiffness than the actual behavior during the first path. This fact led to even 100% greater slips around the pinned support. However, if secant stiffness is implemented when approaching the load-slip curve, a better approximation of the slips is

obtained. Finally, it must be mentioned that the underestimation of slips around the vertexes of the tri-linear model does not lead to noticeable differences in the final results.

2.3 Numerical analyses of continuous composite beams.

The short-term analysis is carried out by increasing the load up to the beam failure. An overall of 13860 beams (10764 for Class 1, and 3096 for Class 2) are modeled by using 40 finite elements. The beams are divided into segments of a length equal to L/60. There are finite elements with a length of L/60, 2xL/60 and 3xL/60, depending on the location. Those located near the supports or mid-span are the shortest ones in order to achieve higher precision where the shear or bending moment is greater and where they change more rapidly. Load and displacement control are used. The convergence tolerance for each load step is considered equal to 0.1%. If the error tolerance value is exceeded, the load step is automatically reduced by a factor of 100 until the convergence is reached. The analysis keeps increasing the load factor in a 6% at each load step and it ends when the collapse condition is attained. Therefore, we will consider that the collapse of the beam occurs whether the maximum strain, ε_{ru}, is achieved at the reinforcement bars or when the maximum rotation capacity is achieved due to local buckling i n the profile steel, which implies that the critical buckling strain is reached.

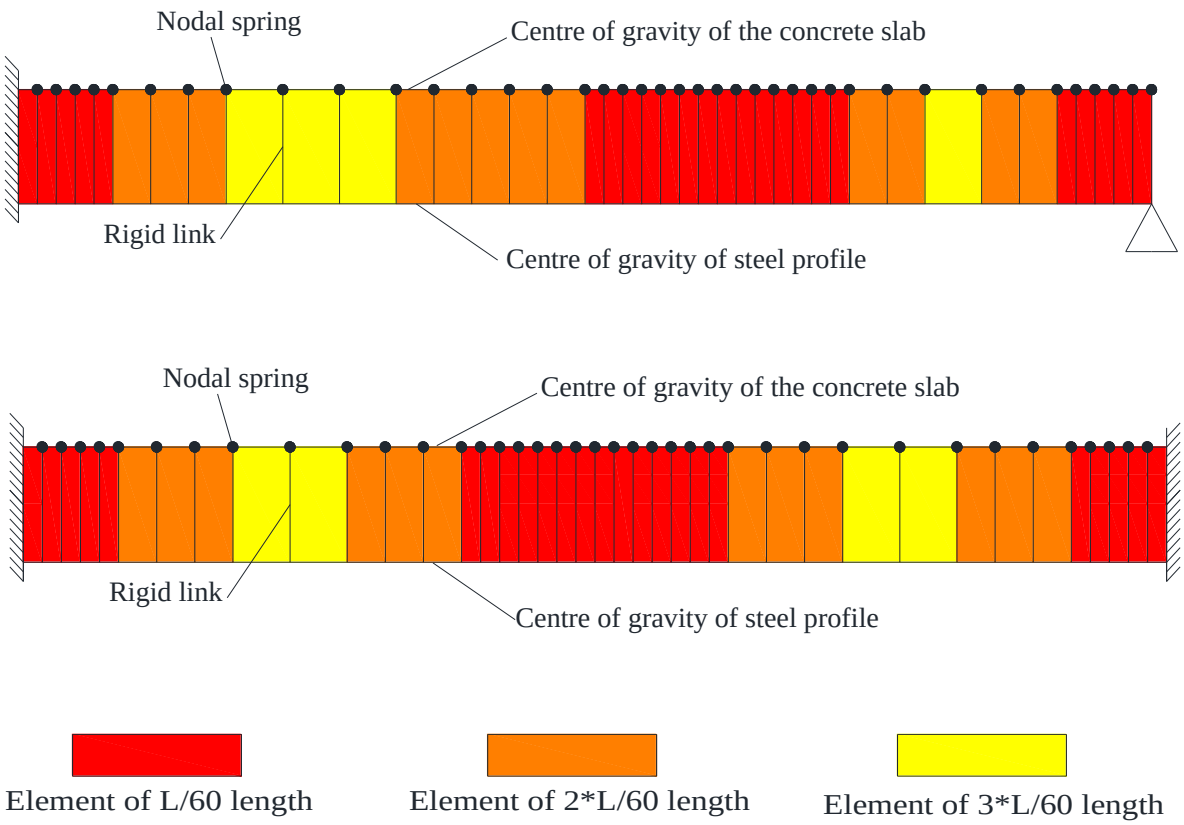

Figure 2.7: Numerical Finite Element model for propped cantilevers and fixed end beams, respectively.

The mesh for the model consists of 41 nodes which represent the center of gravity of the steel profile (from node 1 to 41), 41 nodes which represent the center of gravity of the concrete slab (from nodes 42 to 82) and then 41 more auxiliary nodes to implement the idealization of the shear connection system (from 83 to 123). The lasts ones are coincident with the ones in the concrete slab at the beginning of the analysis. Then, as the beam start to deflect, they have relative horizontal displacements. Therefore, if the lasts 41 nodes are connected with the ones within steel profile with rigid links, i.e. the relative displacement between them is 0, the difference in the displacements between the nodes that forms the springs will be the slip:

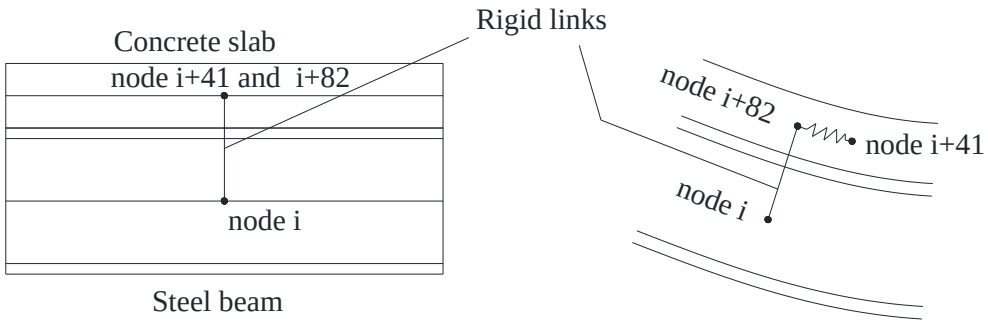

Figure 2.8: Development of slips during the analysis.

Finally, mention that the method used to reach the solution at each step within each increment of load is the Newton Raphson Modified. However, the stiffness matrix is modified every 2 steps in order to achieve the convergence in a quicker way.

3. Evaluation of allowable moment redistribution.

The work with the elastic bending moment envelope with limited redistribution allows the designer to take into consideration the plastic behaviour of the composite beam. It avoids the necessity of carrying out difficult nonlinear analyses. Therefore, the designer is able to optimize the behaviour of the beam, fully exploiting its strength and deformation capacities of all the materials. As a consequence, more economic designs are achieved when the designer works with the redistributed envelope. This envelope consists on reducing the maximum elastic moment at hogging regions (inner supports generally), while increasing the maximum elastic moment at sagging regions to satisfy the equilibrium with external loading. However, the maximum percentage of moment redistribution at ULS is limited by the rotation capacity within the critical sections such as inner supports. During the next sections the method followed to compute the allowable moment redistribution values is explained.

3.1. Class-1 cross steel sections.

At ULS, the permissible moment redistribution can be computed as a function of the maximum load, q_u, that the beam can support (Gattesco and Cohn 1989). That maximum load depends on the type of collapse that the beam experiences. For class-1 cross sections, we can have two different types of collapse: due to "ultimate rotation" or due to "mechanism formation". The loads under which these collapses occur are going to be named as q_{u1} and q_{u2}, respectively.

The first type of collapse occurs due to the attainment of the ultimate rotation capacity. It is reached when the critical local buckling strain is attained at steel profile under compression or the elongation at reinforcement rises up to the limit (2.5%). This collapse is common for all type of steel sections that are considered in this research. The other type of collapse is exclusively considered for class-1 steel sections because they are the unique that, as Eurocode 4 (CEN 2004b) states, can develop a mechanism without being previously affected by local buckling. These types of sections can form enough plastic hinges with enough rotation capacity to form a mechanism without reduction of the resistance. Since the plastic moment resistance is greater at mid-span than at the inner supports (hogging plastic moment), the firsts hinges are developed at supports followed by the formation of the hinges at mid-span, and consequently, the formation of the mechanism that leads to the failure of the composite beam. Consequently, the actual collapse load will be the smaller of both of them.

3.2. Class-2 cross steel sections.

The class-2 steel sections can reach the plastic moment of resistance at interior supports. They can develop a first hinge in hogging moment areas. However, the local buckling phenomena lead to a limiting rotation capacity which avoids the development of a mechanism. Therefore, the collapse due to a mechanism formation is not possible because the beam will fail before due to local buckling.

3.3. Allowable moment redistribution due to rotation capacity collapse.

The ultimate load, q_{u1}, is determined by carrying out a nonlinear analysis up to failure of the beam. This analysis is performed with the numerical model described previously, and carried out with ADAPTIC for both, propped cantilevers and fixed-end beams. Therefore, the load can be the one that leads to any of the following cases:

1- Local buckling at steel profile under compression.

2- Maximum elongation at reinforcing steel.

3- The maximum load reached during the analysis.

In other words, as shown in Figure 3.1, if the maximum load is attained before any of the 2 first situations, q_{u1} will be the maximum load reached in the analysis. On the contrary, as shown in Figure 3.2, if the maximum load reached in the analysis is attained after happening any of the 2 first cases, we must consider that the failure has already happened due to attainment of the rotation capacity (attainment of the limit strain). Therefore, in that case, the ultimate load would be the one that leads to the attainment of either the local buckling strain or the maximum elongation of reinforcement (always taking into account which of both situations occurs firstly).

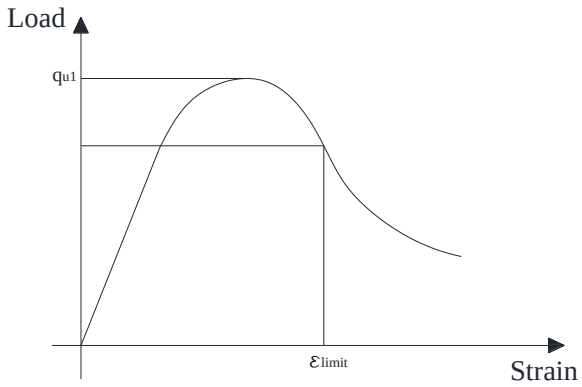

Figure 3.1: Ultimate load value when the strain limit is attained after the maximum load.

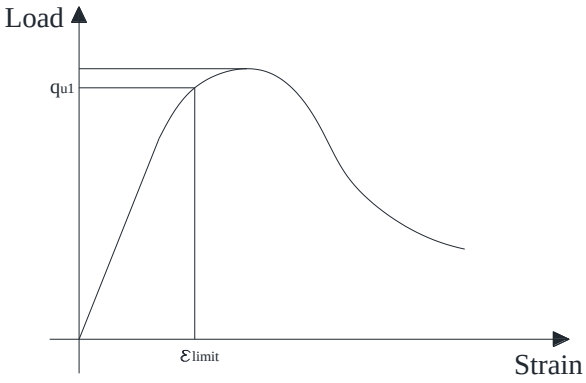

Figure 3.2: Ultimate load value when the strain limit is attained before the maximum load.

The strain limit is understood as the lesser of:

- Strain limit for reinforcement. As mentioned previously, we are working with low ductility reinforcement [εru≥2.5%, class A according to Comite Euro-International du Beton (CEB) 1993]. Therefore, $\varepsilon_{lim.reinf.}$=2.5%. However, the influence of higher ductile steel will be also analysed.

- Strain limit for the structural steel in compression. This limit is the strain that leads the steel profile to suffer from local buckling. According to recent research carried out by Gardner et al. (2013) (under publication), it can be calculated as follows:

$$\varepsilon_{lim.steel} = \varepsilon_{cm} = \frac{0.25}{\overline{\lambda_p}^{3.6}}\varepsilon_y \leq 15\varepsilon_y \tag{3}$$

where $\overline{\lambda_p}$ for plate elements is defined as:

$$\overline{\lambda_p} = \sqrt{\frac{f_y}{\sigma_{cr}}} = \frac{\sqrt{12(1-\nu^2)}\sqrt{235}}{\pi\sqrt{E}\sqrt{k_\sigma}}\left(\frac{b}{t\varepsilon}\right) \tag{4}$$

where σ_{cr} is the elastic critical buckling stress of the plate element, b and t are the plate width and thickness respectively, E is the Young's modulus, ν is Poisson's ratio, $\varepsilon = \left(235/f_y\right)^{1/2}$, and k_σ is the buckling coefficient allowing for differing loading and boundary conditions. The value of the last one is obtained from Table 3.1 and Table 3.2. For flange in compression it is 0.43, and for the web it is 4, when it is all under compression. When the web has a part in tension and a part in compression, this parameter depends on the position of the neutral axis:

$$K_\sigma = 7.81 - 6.29\psi + 9.78\psi^2 \tag{5}$$

Table 3.1: Local buckling coefficient for external compression elements.
Eurocode 3 (Part 1-5, CEN 2005).

Stress distribution (compression positive)	Effective[P] width b_{eff}
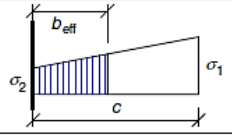	$1 > \psi \geq 0$: $b_{eff} = \rho\, c$
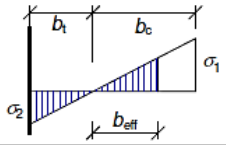	$\psi < 0$: $b_{eff} = \rho\, b_c = \rho\, c\,/\,(1-\psi)$

$\psi = \sigma_2/\sigma_1$	1	0	-1	$1 \geq \psi \geq -3$
Buckling factor k_σ	0,43	0,57	0,85	$0{,}57 - 0{,}21\psi + 0{,}07\psi^2$

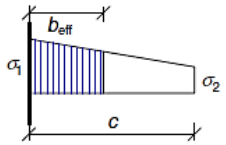	$1 > \psi \geq 0$: $b_{eff} = \rho\, c$
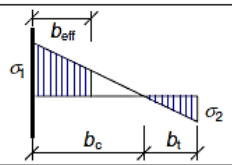	$\psi < 0$: $b_{eff} = \rho\, b_c = \rho\, c\,/\,(1-\psi)$

$\psi = \sigma_2/\sigma_1$	1	$1 > \psi > 0$	0	$0 > \psi > -1$	-1
Buckling factor k_σ	0,43	$0{,}578\,/\,(\psi + 0{,}34)$	1,70	$1{,}7 - 5\psi + 17{,}1\psi^2$	23,8

Table 3.2: Local buckling coefficient for internal compression elements.
Eurocode 3 (Part 1-5, CEN 2005).

Stress distribution (compression positive)	Effective[p] width b_{eff}
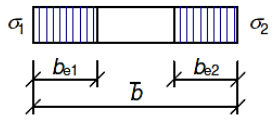	$\psi = 1$: $b_{eff} = \rho\ \bar{b}$ $b_{e1} = 0{,}5\ b_{eff}$ $b_{e2} = 0{,}5\ b_{eff}$
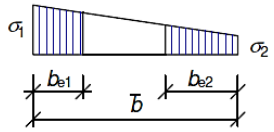	$1 > \psi \geq 0$: $b_{eff} = \rho\ \bar{b}$ $b_{e1} = \frac{2}{5-\psi} b_{eff}$ $b_{e2} = b_{eff} - b_{e1}$
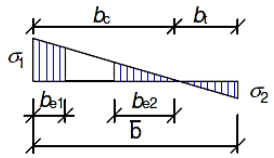	$\psi < 0$: $b_{eff} = \rho\ b_c = \rho\ \bar{b} / (1-\psi)$ $b_{e1} = 0{,}4\ b_{eff}$ $b_{e2} = 0{,}6\ b_{eff}$

$\psi = \sigma_2/\sigma_1$	1	$1 > \psi > 0$	0	$0 > \psi > -1$	-1	$-1 > \psi > -3$
Buckling factor k_σ	4,0	$8{,}2 / (1{,}05 + \psi)$	7,81	$7{,}81 - 6{,}29\psi + 9{,}78\psi^2$	23,9	$5{,}98\ (1 - \psi)^2$

where ψ is considered to be the ratio between the maximum stress in tension over the maximum stress in compression. However, since it is a parameter which defines the part of the web which is in compression, and adaptic give us the strains at bottom and top fibers of the steel member at each load step, ψ .has been considered as the tensile over compressive strain ratio.

Once we have computed the ultimate load, we can proceed to calculate the permissible moment redistribution. The elastic hogging moment at the fixed support can be calculated using the following equation:

$$M_{e1} = -\frac{q_{u1} l^2}{\lambda} \mu \tag{6}$$

where λ is a coefficient depending on the type of restraints at the end of the beam and μ is another one depending on the type of beam. Since the stiffness of the beam changes whether it is analyzed in sagging or hogging bending moment region, it must be accounted with the ratio ν (ratio between flexural stiffness under sagging and hogging bending moment). It must be also taken into account the proportion of those regions through the coefficient κ which is the ratio between the length under hogging bending moment and the whole length. The following equations can be derived using analytical methods of the theory of elasticity (Gattesco et al., 20120):

- Propped cantilevers (λ=8, κ=0.25):

$$\mu = \frac{1+\kappa^2(\nu-1)(6-8\kappa+3\kappa^2)}{1+\kappa(\nu-1)(3-3\kappa+\kappa^2)} \tag{7}$$

- Fixed-end beams (λ=12, κ=0.20):

$$\mu = \frac{1+2\kappa^2(\nu-1)(3+2\kappa)}{1+2\kappa(\nu-1)} \tag{8}$$

Once the elastic bending moment M_{e1} at the support has been calculated, the allowable moment distribution can be calculated from the Equation (9). It shows that the reduced hogging moment, M_{p1}, due to section plasticization for class-1 and class-2 sections, is equal to the reduction factor $(1-y_{u1})$ multiplied by the elastic hogging moment, M_{e1}, which is expressed as in Equation (6).

$$\frac{M_{p1}}{(1-y_u)} = M_{e1} = \frac{q_{u1}l^2}{\lambda}\mu \tag{9}$$

The resistant hogging moment, M_{p1}, is evaluated accordingly to Eurocode 4 (CEN 2004b). Finally, the allowable moment redistribution percentage due to attainment of ultimate rotation capacity at hogging moment region (inner supports) can be calculated as follows:

$$y_{u1} = 1 - \frac{M_{p1}}{M_{e1}} = 1 - \frac{M_{p1}}{q_{u1}l^2}\frac{\lambda}{\mu} \tag{10}$$

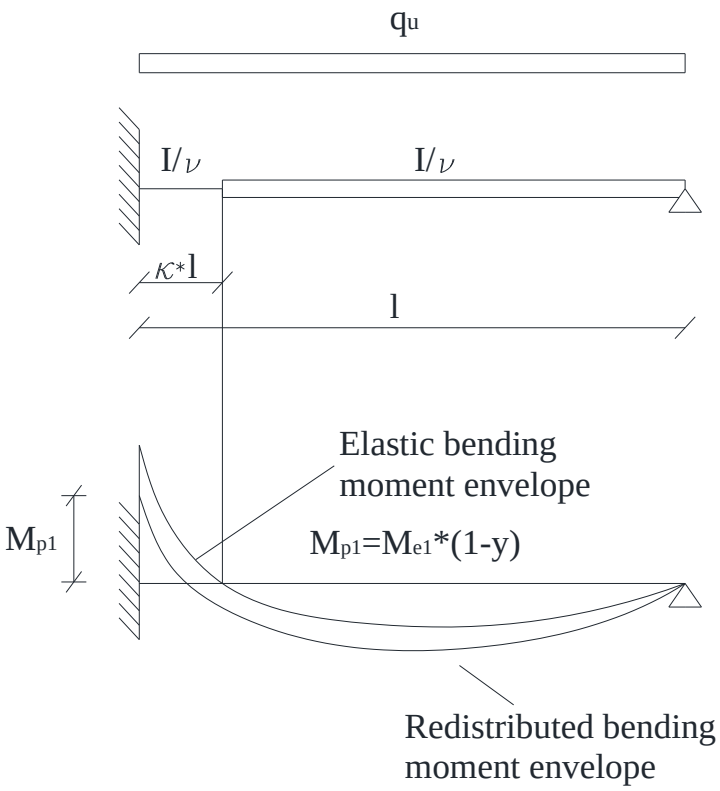

Figure 3.3: Redistribution of elastic moments at propped cantilevers.

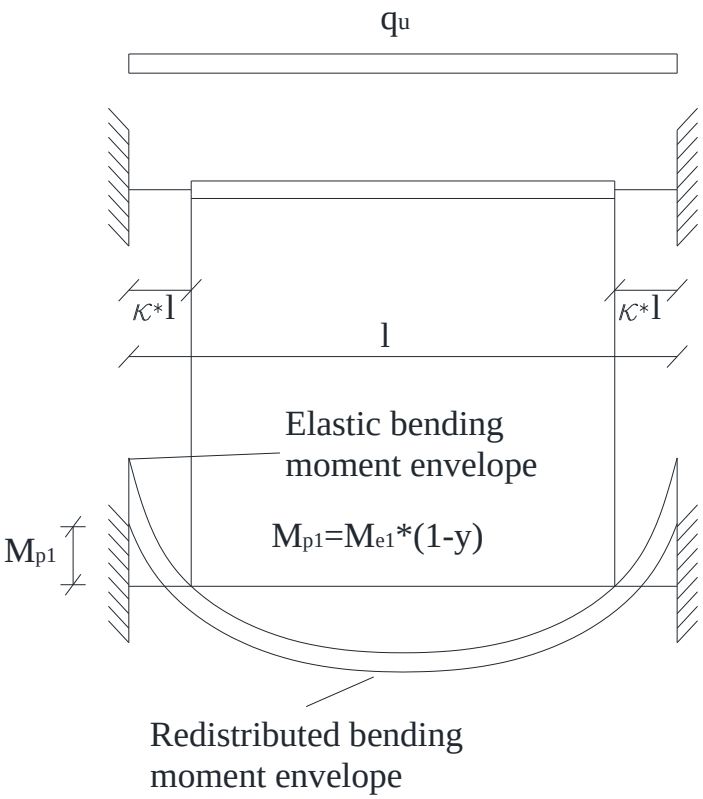

Figure 3.4: Redistribution of elastic moments at propped cantilevers.

3.4. Allowable moment redistribution due to mechanism collapse.

This one is only computed for class-1 cross sections. The ultimate load, q_{u2}, can be simply calculated doing equilibrium analyses of the beam when the plastic resistance moments are attained at enough critical sections to form a mechanism. In order to carry out this analysis, apart from calculating the plastic hogging moment, M_{p1}, the plastic sagging moment, M_{p2}, has to be obtained too. Once it has been done, the procedure to calculate q_{u2} is based on the limit equilibrium equations (Gattesco and Cohn, 1989):

$$\begin{cases} \xi M_{p1} + M_{p2} = \dfrac{q_{u2} l^2}{2} \xi (1-\xi) & \text{(for propped cantilevers)} \\ M_{p1} + M_{p2} = \dfrac{q_{u2} l^2}{8} & \text{(for fixed end beams)} \end{cases} \tag{11}$$

where ξ is the distance between the section of maximum sagging bending moment and the pinned support. Solving Equations (11), and denoting with α the ratio between the hogging plastic moment over the sagging one, M_{p1}/M_{p2} we can obtain the ultimate load as follows:

$$\begin{cases} q_{u2} = \dfrac{4M_{p2}}{l^2}\left(1 + \dfrac{\alpha}{2} + \sqrt{1+\alpha}\right) & \text{(for propped cantilevers)} \\ q_{u2} = \dfrac{8M_{p2}}{l^2}(1+\alpha) & \text{(for fixed end beams)} \end{cases} \tag{12}$$

Finally, substituting Equations (12) within the Equation (11), we obtain the percentage of permissible redistribution for mechanism collapse for class-1 steel sections:

$$\begin{cases} y_{u2} = 1 - \dfrac{2\alpha}{\left(1 + \dfrac{\alpha}{2} + \sqrt{1+\alpha}\right)}\dfrac{1}{\mu} & \text{(for propped cantilevers)} \\ y_{u2} = 1 - \dfrac{3\alpha}{2(1+\alpha)}\dfrac{1}{\mu} & \text{(for fixed end beams)} \end{cases} \tag{13}$$

Therefore, since class-1 sections can collapse due to both, mechanism or attainment of rotation capacity, class-1 sections will have two possible percentages of allowable redistribution. Consequently, the percentage of allowable moment redistribution that must be considered is the smaller of both.

4. Parametric analysis

The domain of allowable moment redistribution was computed analyzing a wide range of steel-concrete composite beams under uniformly distributed load. Once done that, the influence of different types of loading on the redistribution was analysed for one case and then extrapolated for the rest. The short-term analysis (ULS) was carried out for both, propped cantilevers and fixed end beams. The design of the beams was subjected to both full and partial shear connection (Eurocode 4, CEN 2004b). Therefore, different grades of shear connection such as 100%, 75% and 50% were considered. Three different steel grades, S235, S275 and S355, are considered for steel profile, as well as 2 different characteristic compressive cylinder strength (f_{ck}), 30 and 40 N/mm^2, for concrete. For the reinforcing bars, yield strength of 430N/mm^2 was assumed, as well as low ductility steel with uniform elongation at maximum load equal to 2.5%. However, the influence of higher ductile steel grades will also be analysed. Class 1 and 2 (Eurocode 3, CEN 2005) for steel sections are used in the analysis. Finally, headed studs of 19mm of shank diameter and 125mm of overall nominal height are considered with a specified ultimate tensile strength of the material equal to 510N/mm^2. Following the Eurocode 4 (CEN 2004b) rules, the design resistance for a unique headed stud welded to the top flange of the steel member can be obtained from the smaller of the following two numbers:

$$P_{rd} = \frac{0.8 f_u \pi\, d^2/4}{\gamma_v} \qquad P_{rd} = \frac{0.29 \alpha d^2 \sqrt{f_{ck} E_{cm}}}{\gamma_v} \tag{14}$$

where α is defined as:

$$\alpha = 0.2\left(\frac{h_{sc}}{d} + 1\right) \quad for \quad 3 \le h_{sc}/d \le 4$$
$$\alpha = 1 \quad for \quad h_{sc}/d > 4 \tag{15}$$

and:

- γ_v is the partial factor;

- d is the diameter id the sank of the stud, 16mm ≤ d ≤ 25mm;

- f_u is the specified ultimate tensile strength of the material of the stud but not greater than 500N/mm^2;

- f_{ck} is the characteristic cylinder compressive strength of the concrete at the age considered, of density not less than 1750Kg/m^3;

- h_{sc} is the overall nominal height of the stud.

Therefore, we have a resistance of 84.1KN for the studs of the beams with a slab made of concrete with 30 N/mm^2 compressive resistance and 90.7 for the studs of the rest of the beams.

4.1 Choice of geometrical properties.

4.1.1 Choice of geometrical properties for the steel cross sections.

Steel sections from UKB Corus' catalogue were used (Corus Construction & Industrial, 2007):

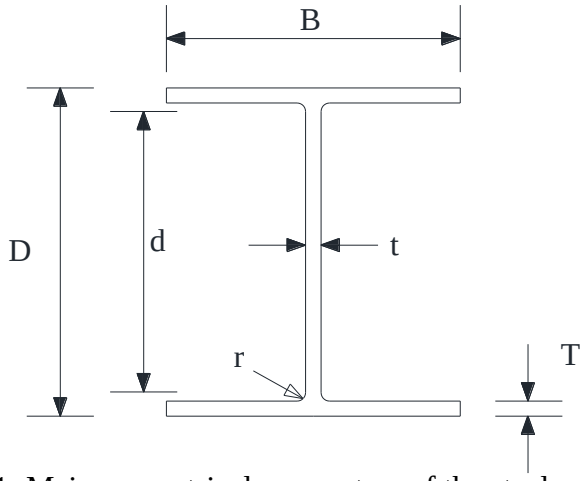

Figure 4.1: Main geometrical parameters of the steel cross sections.

Table 4.1: Main geometrical parameters of the 16 steel cross sections used.

Serial Name	Mass (Kg/m)	Depth of section	Width of section	Thickness of web	Thickness of flange	Root Radius
		D (mm)	**B** (mm)	**t** (mm)	**T** (mm)	**r** (mm)
1016x305x487	486.7	1036.3	308.5	30	54.1	30
1016x305x437	437	1026.1	305.4	26.9	49	30
1016x305x393	392.7	1015.9	303	24.4	43.9	30
1016x305x349	349.4	1008.1	302	21.1	40	30
1016x305x314	314.3	999.9	300	19.1	35.9	30
914x419x388	388	921	420.5	21.4	36.6	24.1
610x305x238	238.1	635.8	311.4	18.4	31.4	16.5
533x312x272	273.3	577.1	320.2	21.1	37.6	12.7
533x312x219	218.8	560.3	317.4	18.3	29.2	12.7
533x312x182	181.5	550.7	314.5	15.2	24.4	12.7
533x210x138	138.3	549.1	213.9	14.7	23.6	12.7
457x191x161	161.4	492	199.4	18	32	10.2
457x191x133	133.3	480.6	196.7	15.3	26.3	10.2
457x191x106	105.8	469.2	194	12.6	20.6	10.2
457x191x98	98.3	467.2	192.8	11.4	19.6	10.2
406x178x85	85.3	417.2	181.9	10.9	18.2	10.2

In order to analyse a wide range of different beams, the depth of those beams, D, varies within the range from 1036.3mm to 417.2mm. An overall of 16 different cross steel sections have been modeled. The main features of these beams are summarized in the previous table.

4.1.2 Choice of the rest geometrical properties.

The choice of the beams' parameters was done in order to analyze real steel-concrete composite beams. The concrete slab depth, h_C, was considered equal to 150,200 and 250mm. The concrete width was related to the span of the beam. Two more widths were taken into account multiplying the previous one by two reduction factors, 5/6 and 2/3, respectively. The purpose of that is to include cases with smaller spacing between beams. However, the effective width rules specified at Eurocode 4 (CEN 2004b) were taken into account to avoid overestimation of the strength of the concrete part. Therefore, the slab width is the lesser between the effective width and the beam spacing. The area of reinforcement was assumed equal to 0.5%, 1% and 1.5% of the effective area of concrete slab. A cover equal to 30mm from the upper fiber of the concrete slab was assumed. An overall of 2310 propped cantilevers and 2310 fixed end beams were obtained by combining all these factors. Therefore, an overall of 6930 beams for each type are obtained when working with the three different degrees of connection (100%, 75% and 50%). A ratio of 20 between the length and the overall depth was assumed for all beams since this is the average ratio commonly used in composite floor construction.

Some geometric non-dimensional parameters were identified by Johnson and May (1975) to represent the features of the steel-concrete composite beams. They take into account the shape of the steel profile and the concrete slab, the ratios between steel profile and concrete areas, between reinforcement and steel profile areas and the ratio between the span length and the overall depth.

Parameter		min. value	max. value
Slab shape factor	b_c/h_c	7.11	31.63
Concrete-steel depth ratio	d/h	0.10	0.33
Steel profile shape factor	$I_s/A_s h_s^2$	0.15	0.18
Steel-concrete area ratio	A_s/A_c	0.03	0.14
Reinforcement-steel area ratio	A_r/A_s	0.04	0.57
Span-depth ratio	L/h	20	

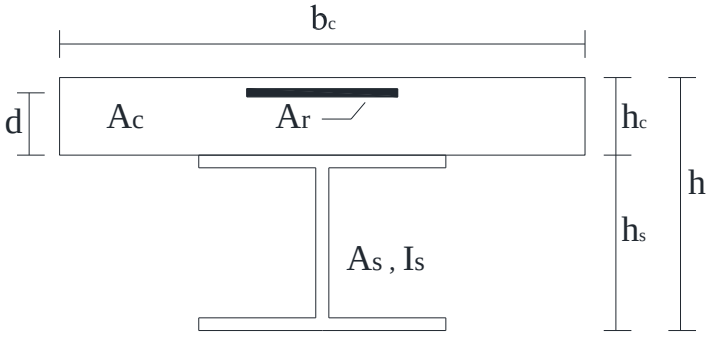

Figure 4.2: Range of variation of non-dimensional geometrical parameters.

Finally, it must be pointed out that beams with no technical interest were removed from the analysis such as those ones with a reinforcement-steel area ratio greater than 0.5 (Gattesco et al., 2010):

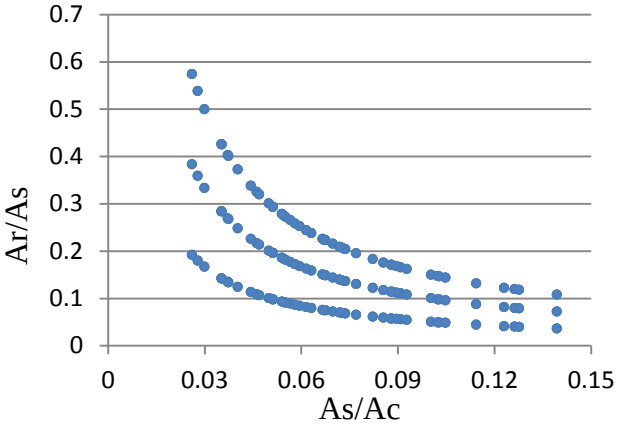

Figure 4.3: Combination of the A_r/A_s ratio with the A_s/A_c ratio for the whole range of beams.

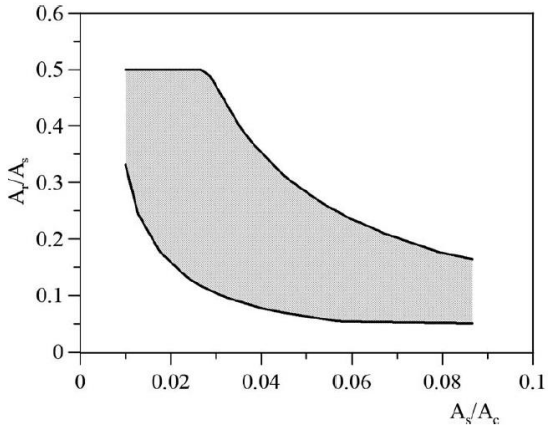

Figure 4.4: Possible range of variation of the A_r/A_s ratio with the A_s/A_c ratio. (Gattesco et. al 2010).

5. Outcomes of the analyses.

This section presents the results obtained for both classes of structural steel and for the different degrees of shear connection between the slab and the steel profile.

The numerical analyses, which were carried out with the numerical procedure described before, allowed obtaining the ultimate load, q_{u1}, for which ultimate rotation capacity is achieved at hogging moment regions due to the attainment of either the ultimate tensile strain at reinforcement bars or the critical local buckling strain at steel member. The ultimate load that causes collapse due to the formation of enough hinges to lead the failure to a mechanism failure, q_{u2}, has been obtained from Equations 11. Then the permissible moment redistribution factor for both ultimate loads has been calculated from Equations (10) and Equations (13), respectively.

5.1 Class-1 cross steel sections.

The outcomes of the analyses for class-1 cross steel sections are shown below. The results are classified in different sections for full shear connection, partial connection with a degree of connection of 75%, and partial shear connection with a degree of connection of 50%, respectively. The limits of permissible moment redistribution established by the Eurocode 4 (CEN 2004b) for Class 1 composite sections and by the American code, AISC 360-05 (AISC 2005), when local and lateral-torsional buckling conditions are attained, are also plotted in the graphs.

5.1.1 Full shear connection.

In Figures 5.1 and 5.2 the permissible moment redistribution percentage due to rotation capacity is plotted against the reinforcement-steel area ratio for ULS requirements and for propped cantilevers (Figure 5.1) and fixed end beams (Figure 5.2). These figures show that the American code's limit (AISC 360-05, AISC 2005) seems to be a good approach for propped cantilevers. Nevertheless, an 8% of the cases from fixed end beams (4% of overall cases) have a permissible redistribution percentage under this threshold. That happens because, at the supports of fixed end beams, the plastic rotation demand is higher than at propped cantilevers' fixed support. For that reason, the elastic bending moment at fixed supports caused by the ultimate load is smaller for fixed end beams than for propped cantilevers. Consequently, in accordance with Equation (10), the percentage of allowable redistribution has to decrease when a given cross section is used within a fixed end beam, or in other words, within an internal span of a continuous beam. Therefore, some sections that are close to the AISC 360-05 limit when they are used within a propped cantilever, fall below the threshold when they are used in fixed end beams.

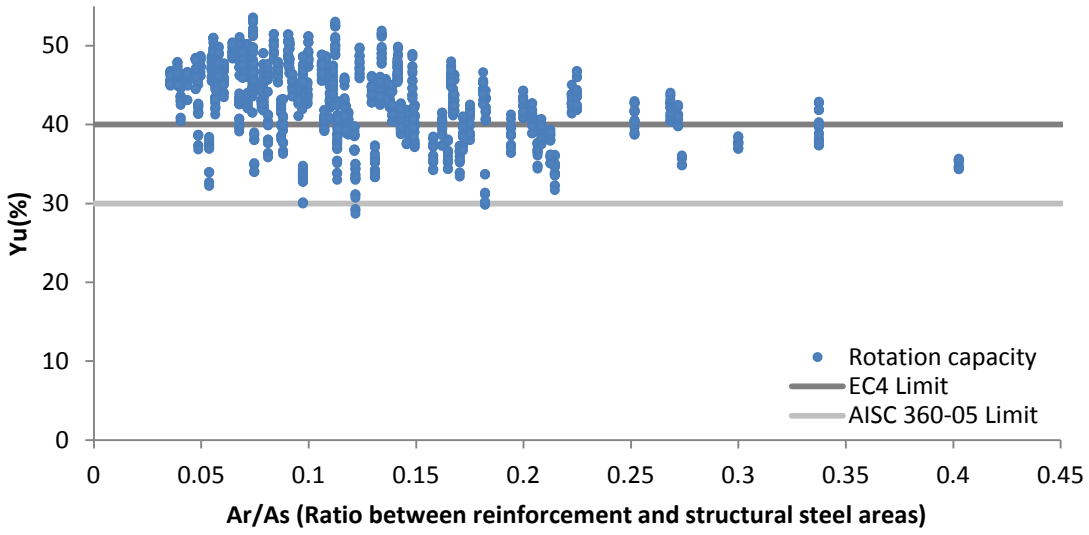

Figure 5.1: Permissible moment redistribution at ULS versus the reinforcement ratio for propped cantilevers.

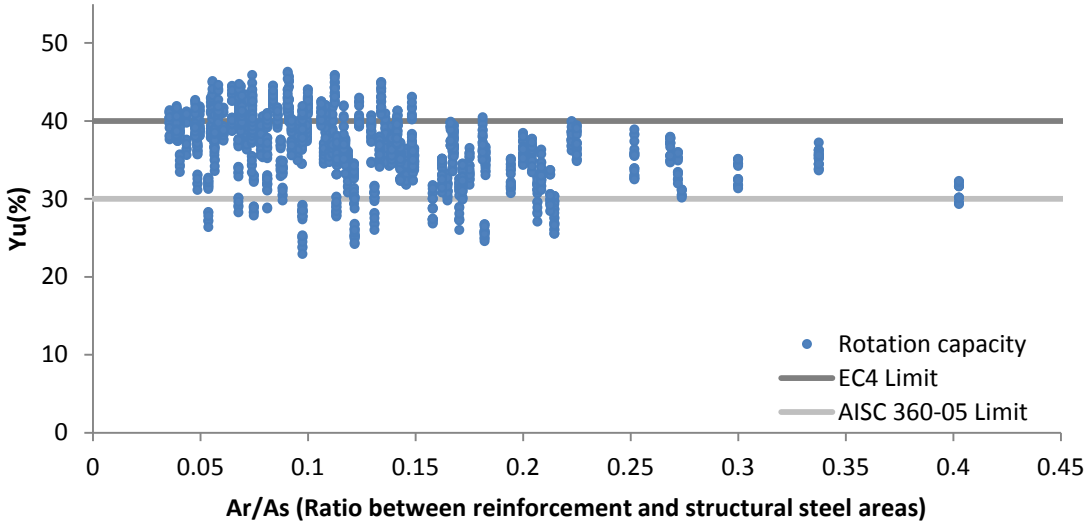

Figure 5.2: Permissible moment redistribution at ULS versus the reinforcement ratio for fixed end beams.

On the other hand, for both, propped cantilevers and fixed end beams, the limit stated by the Eurocode 4 (CEN 2004b) is unconservative because the permissible redistribution percentage of most of the cases analyzed is under this threshold. The reason why this happens is that the Eurocode 3 does not consider local buckling for Class 1 cross steel sections. Therefore, the difference between both codes lies in the fact that when establishing these limits, the American one takes into account the local and lateral-torsional buckling, whereas the Eurocode does not. Consequently, not taking into account this phenomenon leads to an unconservative rule.

The collapse is mainly reached due to the attainment of rotation capacity, since in most of the cases q_{u1} is smaller than q_{u2}. However, in almost 29% of the cases in fixed end beams the failure occurs due to the formation of enough plastic hinges to constitute a mechanism. In

other words, for these cases, q_{u2} is smaller than q_{u1}. On the other hand, all propped cantilevers fail due to rotation capacity attainment. Finally, for propped cantilevers, the 61.35% of cases fail due to attainment of critical local buckling strain at flange, the 35.86% due to the attainment of critical local buckling strain at web, and the 2.79% due to attainment of maximum elongation at reinforcement, ε_{ru}. For fixed end beams, the 52.76% of cases failed due to attainment of critical local buckling strain at flange, the 45.53% due to the attainment of critical local buckling strain at web, and the 1.7% due to attainment of maximum elongation at reinforcement, ε_{ru}.

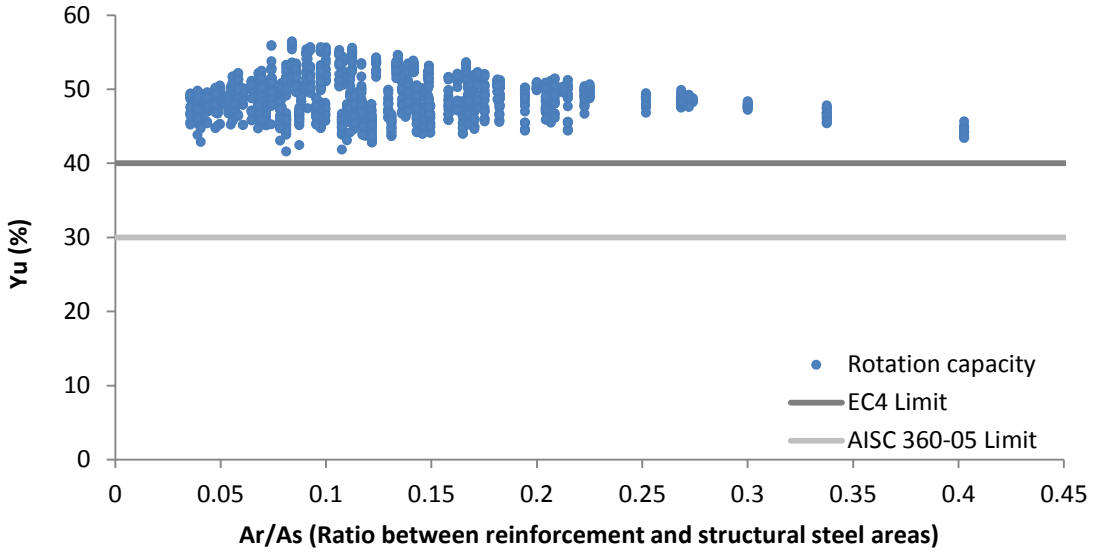

Figure 5.3: Permissible moment redistribution regardless of the local buckling effect for propped cantilevers.

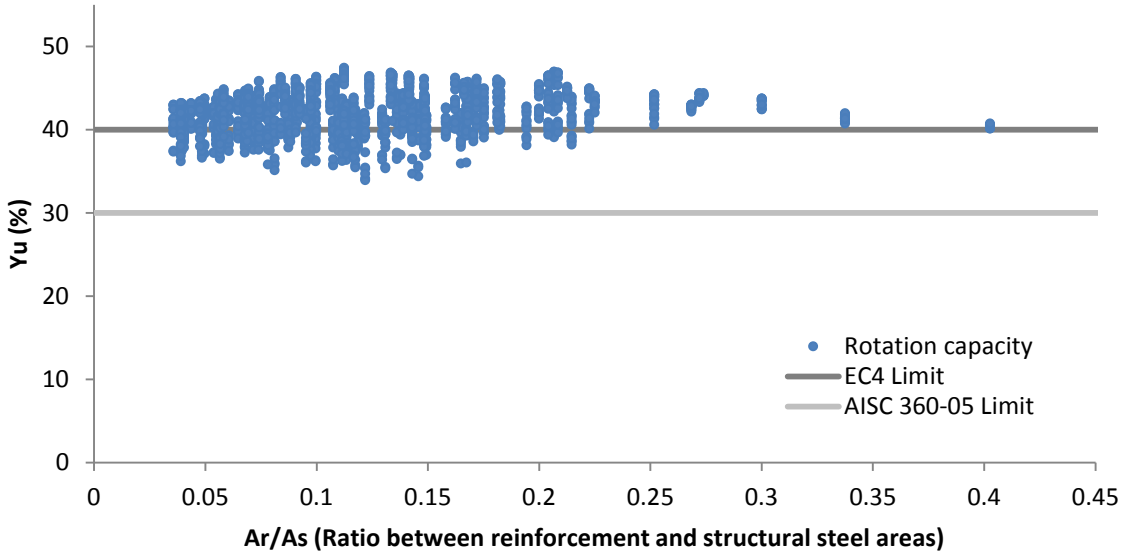

Figure 5.4: Permissible moment redistribution regardless of the local buckling effect for fixed end beams.

The previous graphs (Figures 5.3 and 5.4) were obtained from the numerical results without accounting the local buckling phenomenon. They show the rotation capacity with the only restriction of the attainment of maximum elongation at reinforcement. As can be observed, the limit suggested by Eurocode 4 (CEN 2004b) becomes safe for propped cantilevers when local

buckling is neglected. Nevertheless, for fixed end beams, despite neglecting the local buckling phenomenon, the limit is still unconservative. As shown in Figures5.5 and 5.6, the same occurs if only the collapse due to plastic mechanism formation is considered. The Eurocode 4 (CEN 2004b) limit is conservative for propped cantilevers whereas is not safe for fixed end beams.

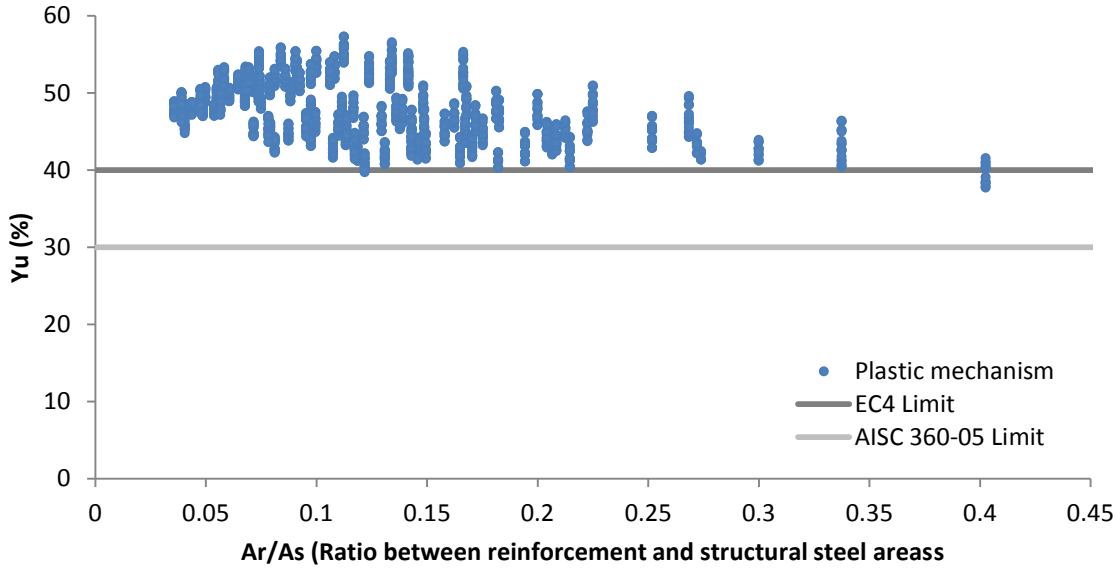

Figure 5.5: Permissible moment redistribution at ULS versus the reinforcement ratio for propped cantilevers.

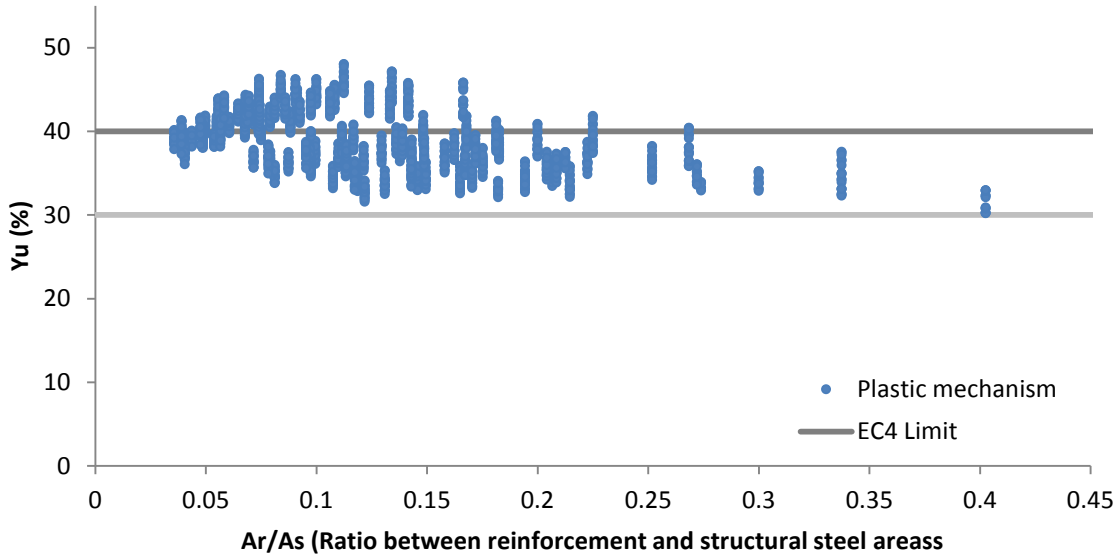

Figure 5.6: Permissible moment redistribution at ULS versus the reinforcement ratio for fixed end beams

5.1.2 Partial shear connection. Degree of connection η=0.75.

The results obtained when the degree of shear connection is 0.75 are shown in Figures 5.7 and 5.8. Comparing these graphs with the ones shown in Figures 5.1 and 5.2 respectiveley, it can be observed that the permissible percentage of redistribution tends to decrease slightly for the overall beams. At this stage, for propped cantilevers, there are only few beams that reach the 50% of redistribution whereas it start to appear few more beams closer to the American code limit (30%). Much more beams are under the Eurocode's thresholds.

The general drop occurs because having two identical beams, subjected to identical loading, but one of them with smaller degree of connection than the other, for the first one, greater slips will be obtained. In other words, this makes the system less stiff, so the deflections are greater and hence the rotations too. The fact of being the rotation greater for the same load implies that the attainment of the rotation capacity's conditions will take place for smaller loads. Summarizing, accordingly with other studies such as Titoum et al. (2009), the ultimate load capacity decreases when degree of connection decreases. Therefore, the redistribution capacity decreases too.

In this case, the limit for moment redistribution stated by Eurocode 4 (CEN 2004b) seems to be unconservative, since there are more beams that have less allowable redistribution than 40%. However, the limit stated by the AISC 360-05 (AISC 2005) is still safe for propped cantilevers, and a little unconservative for fixed end beams (almost 6% of the overall cases have less allowable redistribution percentage than 30%).

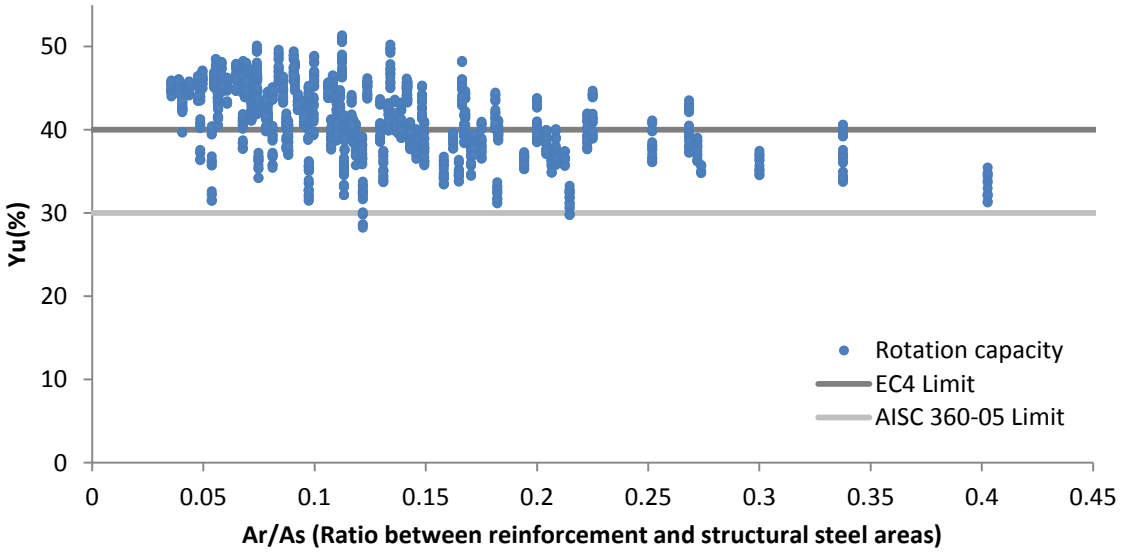

Figure 5.7: Permissible moment redistribution at ULS versus the reinforcement ratio for propped cantilevers.

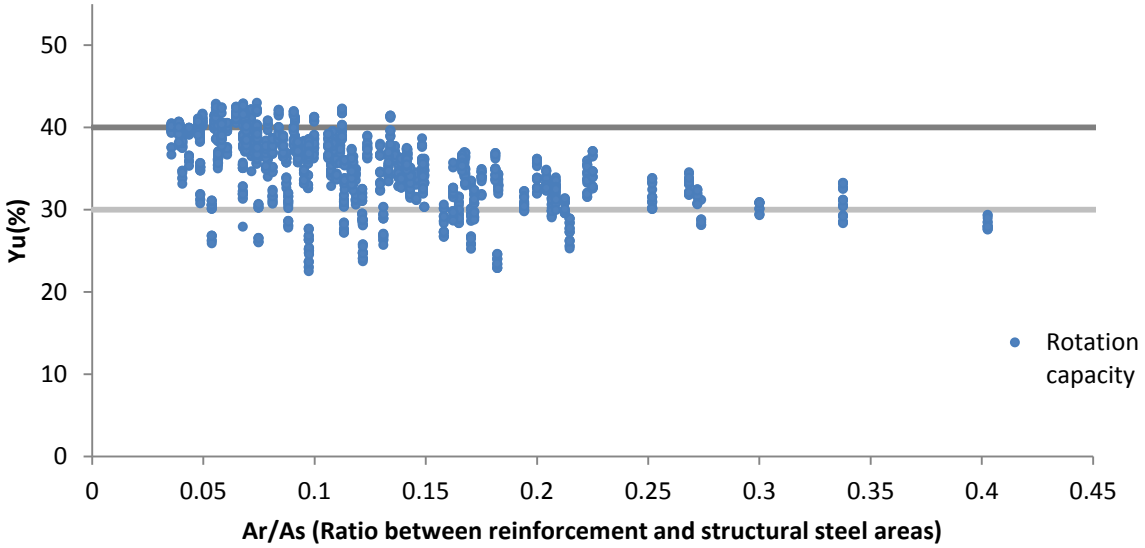

Figure 5.8: Permissible moment redistribution at ULS versus the reinforcement ratio for fixed end beams.

All the failures are due to the attainment of the rotation capacity for propped cantilevers. The percentage of mechanism collapse for fixed end beams drops slightly up to 27.8%. Finally, for propped cantilevers the failures due to maximum elongation at reinforcement decreases up to 0%. The percentage of failures due to attainment of critical local buckling strain at flange increases up to 71.13% and failures due to attainment of critical local buckling strain at web decreases slightly up to 28.87%. The same trend is observed for fixed end beams which experience a fall of reinforcement failures up to 0% while the failures due to attainment of critical local buckling strain at flange increases slightly up to 54.87%. Failures due to local buckling at web are more or less the same (45.13%).

5.1.3 Partial shear connection. Degree of connection η=0.5.

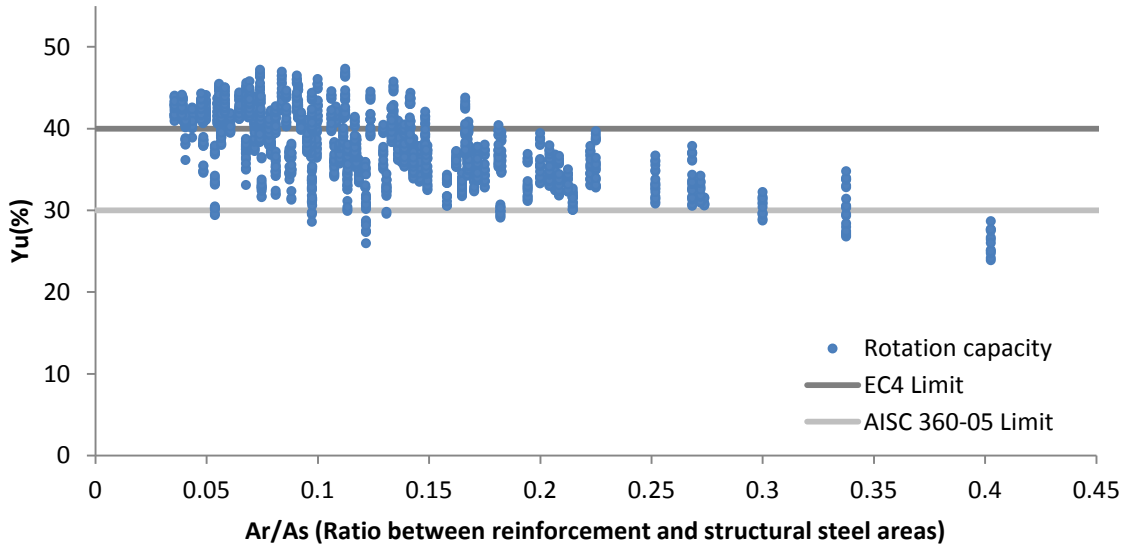

Figure 5.9: Permissible moment redistribution at ULS versus the reinforcement ratio for propped cantilevers.

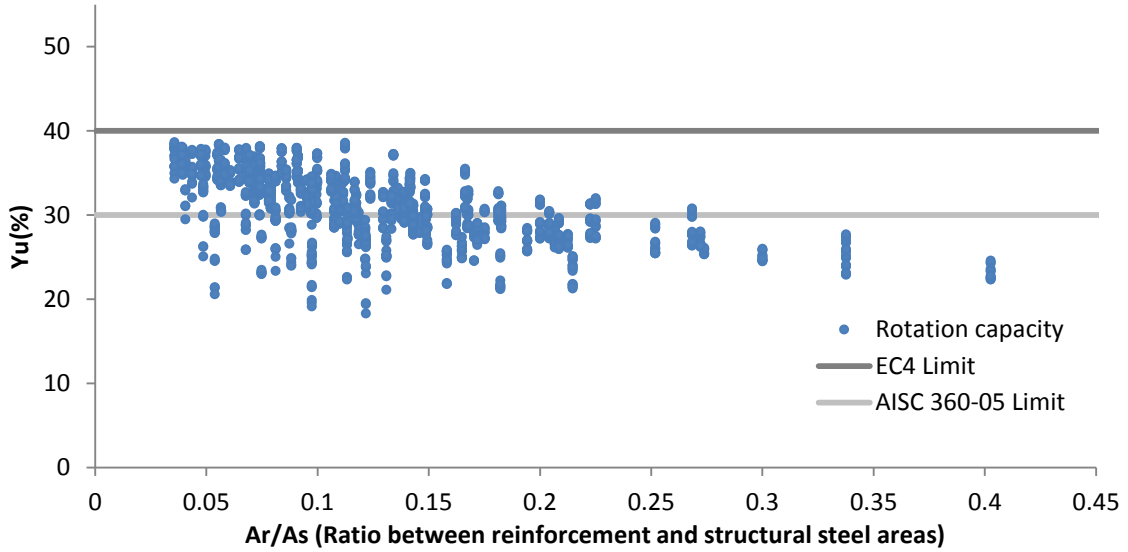

Figure 5.10: Permissible moment redistribution at ULS versus the reinforcement ratio for fixed end beams.

The results obtained when the degree of shear connection is 0.5 are shown in Figures 5.9 and 5.10. It can be observed that the moment redistribution keep falling down when decreasing

the degree of shear connection if we compare these graphs with the ones shown in Figures 5.7, 5.8, 5.9 and 5.10. The same phenomenon explained in the previous section occurs for the beams analysed in the current one. The increase in the slips leads to an increase in the rotation demand at the supports which cause a drop in the allowable redistribution. The limit proposed by the Eurocode 4 (CEN 2004b) is clearly unconservative. The one proposed by the AISC 360-05 (AISC 2005) can be seen as conservative for propped cantilevers but now is undoubtedly unconservative for fixed end beams. All the failures for propped cantilevers are due to attainment of rotation capacity. However, 161 beams, representing a 9% of the overall fixed end beam, failed due to mechanism formation. The rest failed due to attainment of rotation capacity.

Finally, for propped cantilevers and fixed end beams there are not cases of reinforcement failures. The 80.4% of the cases of failures are due to the attainment of local buckling strain at the bottom flange while the 19.6% of cases are due to local buckling at the lower fiber of the web. The percentages for fixed end beams are 70.7% and 29.3%, respectively.

5.2 Class-2 cross steel sections.

The outcomes of the analyses for class-2 cross steel sections are shown below. The results are classified in different sections for full shear connection, partial connection with a degree of connection of 75%, and partial shear connection with a degree of connection of 50%, respectively. The limits of permissible moment redistribution established by the Eurocode 4 (CEN 2004b) for Class 2 composite sections and by the American code, (AISC 360-05, AISC 2005), when local and lateral-torsional buckling conditions are attained, are also plotted in the graphs. As described previously, the European code consider that, due to the features of Class-2 sections, the collapse is only attained due to rotation capacity, since the local buckling phenomena prevent the beam from developing enough hinges to form a mechanism. Therefore, now, unlike for previous cross sections, both codes consider the local buckling phenomena when they suggest the limit. Consequently, for any of the following cases, there will not be any collapse due to mechanism.

5.2.1 Full shear connection.

Figure 5.11 shows that, for propped cantilevers, the limit stated by Eurocode 4 (CEN 2004b) and the AISC 360-05 (AISC 2005), which are the same for Class-2 sections, is not very safe. Almost 23% of the cases do not fulfill the limit. On other hand, for fixed end beams, the same limit is clearly unconservative since a non-negligible number of beams have smaller percentage of redistribution than the one proposed. This number represents 84% of the overall fixed end beams. As mentioned before, the lower redistribution for fixed end beams occurs due to the higher rotation demand at fixed supports.

Finally, for propped cantilevers and for fixed end beams, there are not ruptures neither due to bottom flange buckling nor attainment of reinforcing steel's maximum elongation. All the collapses occur due to web local buckling.

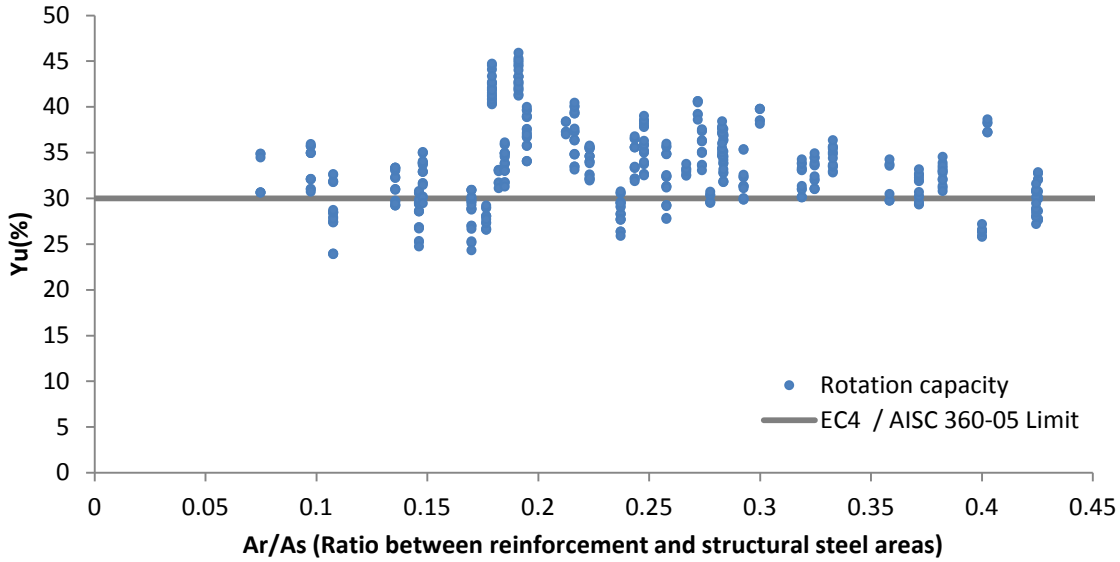

Figure 5.11: Permissible moment redistribution at ULS versus the reinforcement ratio for propped cantilevers.

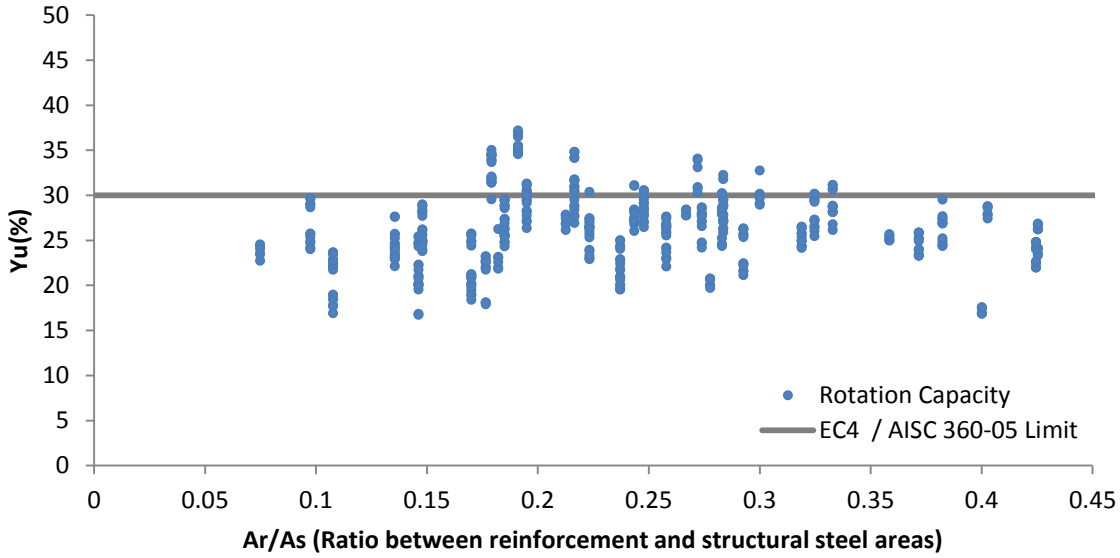

Figure 5.12: Permissible moment redistribution at ULS versus the reinforcement ratio for fixed end beams.

5.2.2 Partial shear connection. Degree of connection η=0.75.

The results obtained when the degree of shear connection is 0.75 are shown in Figures 5.13 and 5.14. Comparing these graphs with the ones showed in Figures 5.11 and 5.12 respectively, the same behaviour as for Class-1 sections can be observed; the allowable redistribution tends to decrease slightly for overall beams. That happens due to the reasons explained within section 5.1.2. As for the case of full connection, the limit stated by both codes is clearly unconservative for propped end beams. Furthermore, the same situation occurs for propped cantilevers for which almost 29% of the cases have less allowable redistribution than the maximum one stated by the codes.

Finally, for propped cantilevers, 2.88% failed due to local buckling at flange. The rest, a 97.12%, were due to web failure. On the other hand, only two of the fixed end beams collapsed due to local buckling at flange and a 99.6% due to local buckling at web. There are not collapses due to attainment of maximum elongation at the reinforcement.

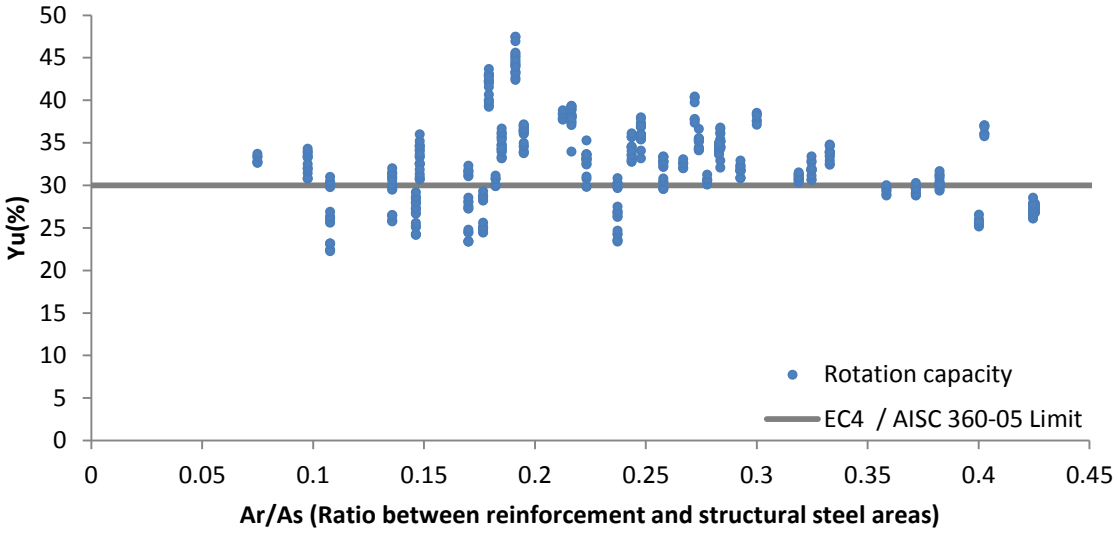

Figure 5.13: Permissible moment redistribution at ULS versus the reinforcement ratio for propped cantilevers.

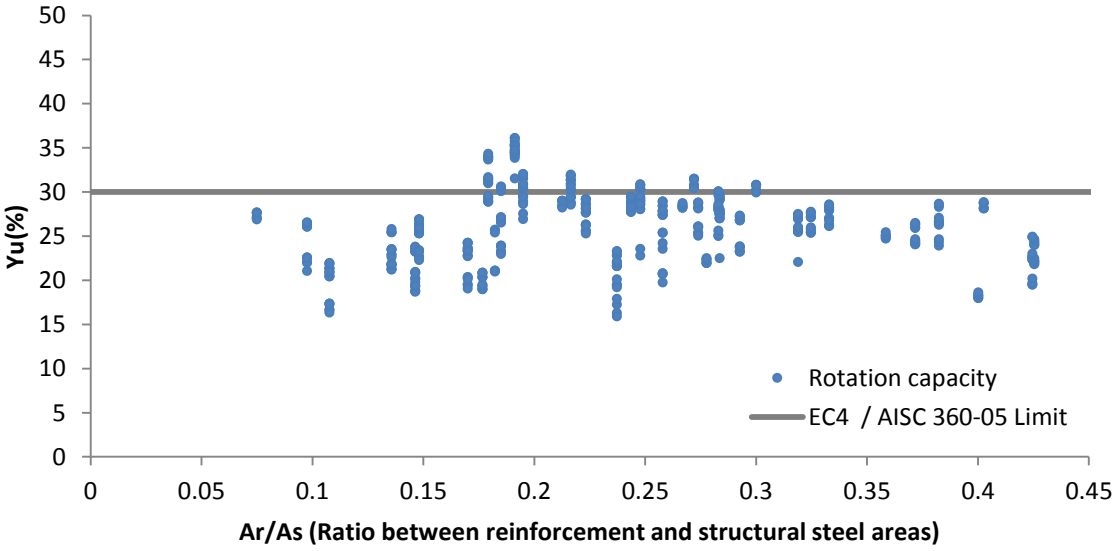

Figure 5.14: Permissible moment redistribution at ULS versus the reinforcement ratio for fixed end beams.

5.2.3 Partial shear connection. Degree of connection η=0.5.

The results obtained when the degree of shear connection is 0.5 are shown in Figures 5.15 and 5.16. The percentage of moment redistribution keeps falling down as the degree of connection decreases. For both classes of beams can be noticed that the change is more noticeable when the degree falls from 0.75 to 0.5 than when the degree falls from 1 to 0.75. The limit proposed by the European and American codes is unconservative for both of these cases. The number of propped cantilevers under the threshold represents almost a 42% from the overall.

Furthermore, the percentage of the fixed end beams that do not fulfill the limit rises up to almost 93%.

Finally, failures due to local buckling at flange increased sharply up to a 43.6% of the propped cantilevers, whereas a 56.4% did it due to local buckling at web. In what fixed end beams is concerned, the 27.52% failed due to local buckling at flange and the rest, a 72.48%, failed due to local buckling at web. No failures due to reinforcing maximum elongation were obtained.

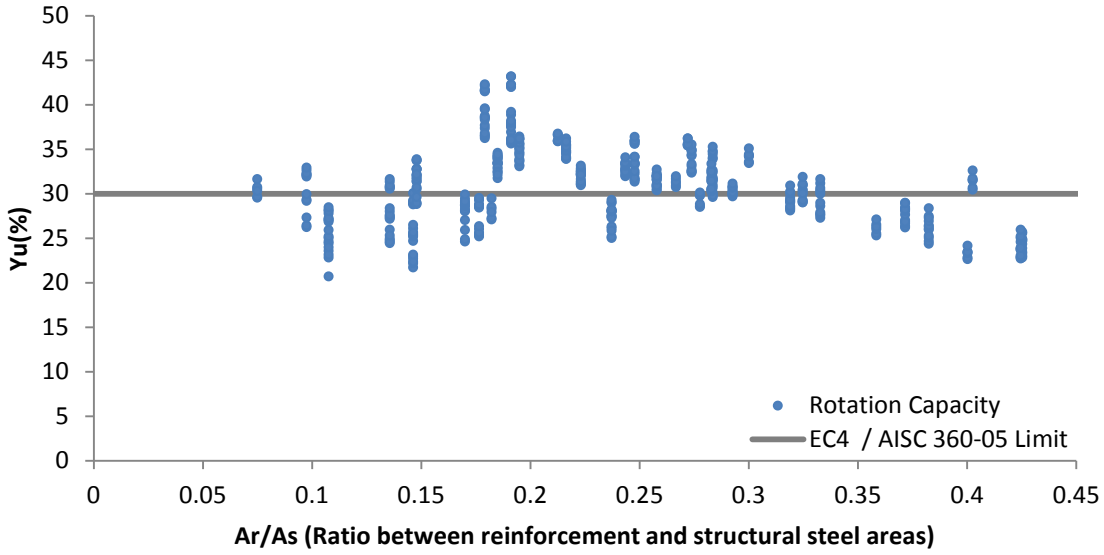

Figure 5.15: Permissible moment redistribution at ULS versus the reinforcement rat io for propped cantilevers.

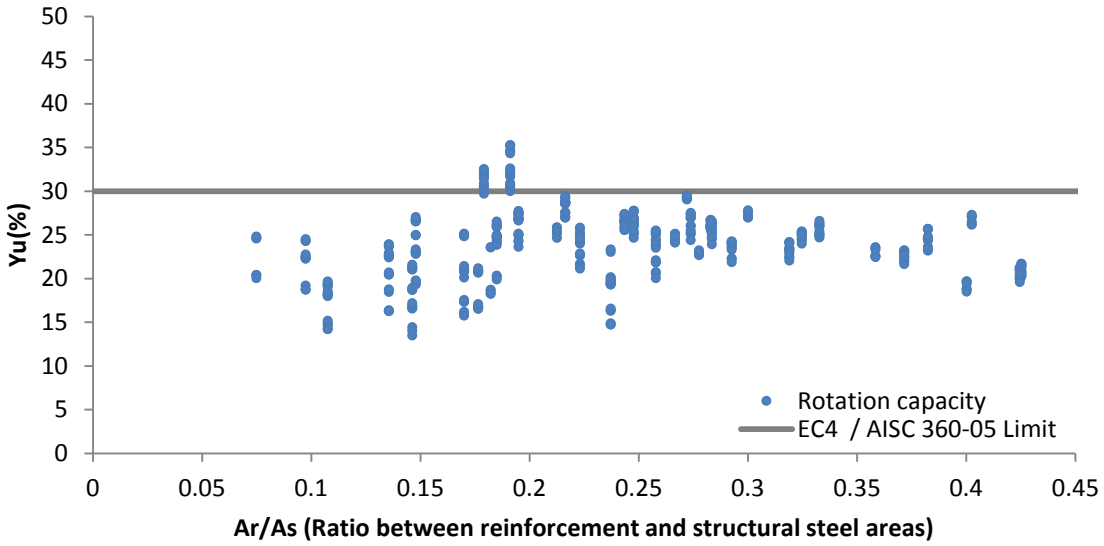

Figure 5.16: Permissible moment redistribution at ULS versus the reinforcement ratio for fixed end beams.

5.3 Influence of type of loading.

The influence of different types of loads were analysed for the cases of Class-1 propped cantilevers with full shear connection. Figure 5.1 shows the case of propped cantilevers under uniformly distributed load (UDL). In the followings graphs (Figures 5.17 and 5.18), the allowable redistribution is showed when the loading consists on 2 point loads at thirds of the whole length (third-point loading) and a concentrated load at midspan, respectively.

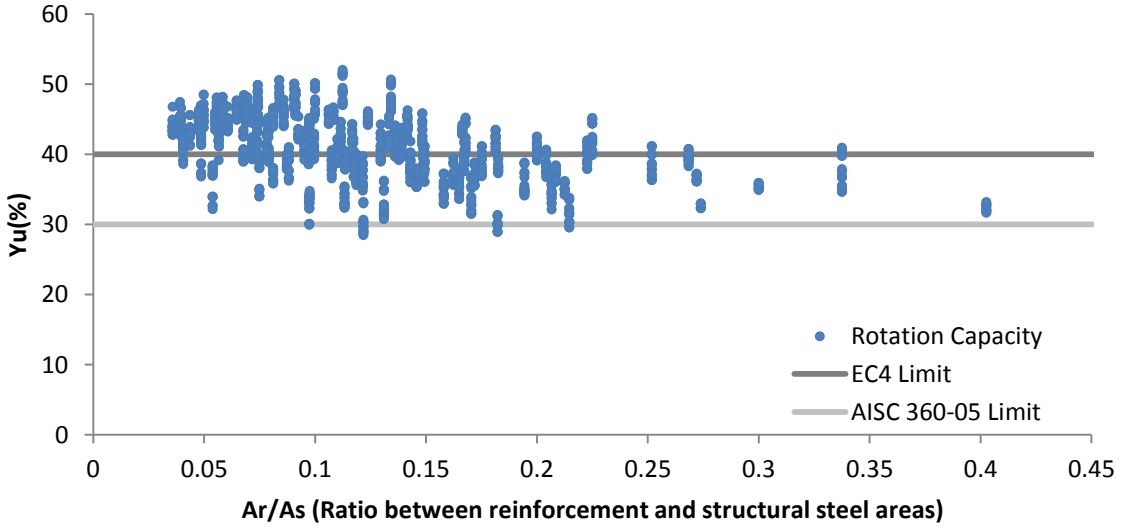

Figure 5.17: Permissible moment redistribution at ULS versus the reinforcement ratio for propped cantilevers under third-point loading.

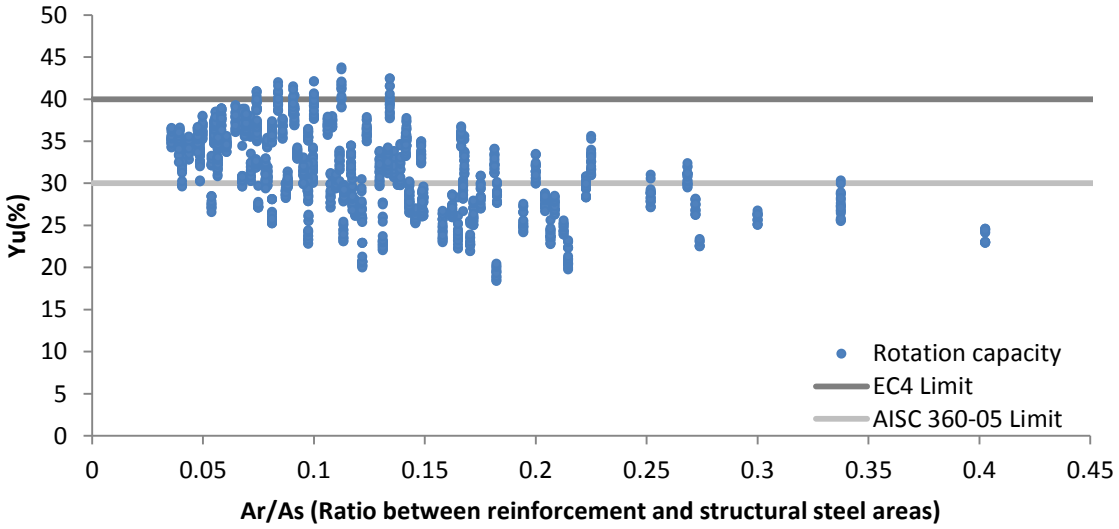

Figure 5.18: Permissible moment redistribution at ULS versus the reinforcement ratio for propped cantilevers under concentrated load at midspan.

According to the three figures mentioned before, one can observe a slightly drop of the allowable redistribution when uniform loading is changed to third-point loading. However, the change from third-point loading to a concentrated point loading entails a sharp reduction

of the permissible moment redistribution. The following graph (Figure 5.19) will help to understand in a better way this phenomenon:

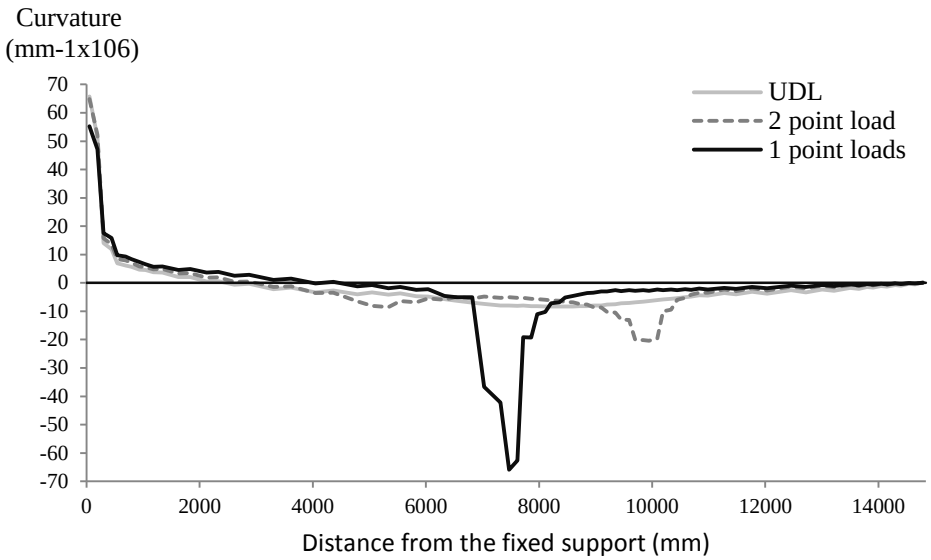

Figure 5.19: Curvature at ultimate limit state due to rotation compatibility of a given beam under the three different types of loading.

The curvature along the whole length of one propped cantilever is plotted for each type of loading. The data was obtained from the output files at Ultimate Limit State due to rotation capacity. As shown in Figure 5.19 for the case of a concentrated load at midspan, a mechanism of plastic hinges has already been formed by the time one of the rotation capacity limitations is attained. Therefore, the rotation at the fixed support increases rapidly when increasing the loading. That fact leads to a quick attainment of the beam's rotation capacity with relatively low loads. Consequently, the elastic bending moment induced at the fixed support at ultimate state due to rotation capacity attainment is lower than for the other cases. As a result, a lower percentage of permissible redistribution is obtained following the next equation:

$$y_{u1} = 1 - \frac{M_{p1}}{M_{e1}} = 1 - \frac{M_{p1}}{q_{u1} l} \frac{\lambda}{\mu} \tag{16}$$

where

$$\begin{cases} \lambda = 3, \kappa = 0.25 & for\ third - point\ loading \\ \lambda = 16/3\,, \kappa = 3/11 & for\ the\ concentrated\ load \end{cases} \tag{17}$$

and μ is obtained from Equation (7).

To sum up, the plastic hinge rotation demand increases as the load is changed from uniform distributed load to a midspan concentrated load. Therefore, at ultimate limit state, the allowable moment redistribution will increase when loading is changed from a concentrated load to a uniformly distributed load.

5.4 Influence of type of reinforcement.

Until now, all the exposed outcomes were obtained assuming low ductility steel for reinforcing bars (εru≥2.5%, class A according to Comite Euro-International du Beton (CEB) 1993). Analyse how different ductile grades of reinforcing steel affect the redistribution was also an objective of this research (ε_{ru}=5% and ε_{ru}=7.5% corresponding to medium and high ductility reinforcement). However, in accordance with the results, the most restrictive condition for the permissible percentage of redistribution was the attainment of local buckling limits. Only for few beams of Class-1 sections with full shear connection, failures due to attainment of maximum elongation in the reinforcement were obtained. Therefore, no failures due to reinforcing were obtained when higher ductility grades were considered. The failures in these cases turned out to be due to local buckling, and the failures due to mechanism formation did not increase.

5.5 Influence of the shear connection degree.

As explained along sections 5.1 and 5.2, analyses with different degrees of shear connection were carried out. Full shear connection (100%), 0.75 and 0.5 degrees of connections were considered. The results showed that the general percentage of redistribution is reduced when the degree of connection decreases. In agreement with experimental research such as the one carried out by Titoum et.al (2009), the numerical results showed that the ultimate load tends to decrease when the degree of connection reduces. This can be explained because the fact of reducing the shear connection leads to greater slips when a beam is under a given load. Therefore, the whole system becomes less stiff, or in other words, more flexible. Consequently, a beam with a lesser shear connection degree will have higher displacements and rotations when they are under the same load. As a result, the rotation capacity restrictions are attained under a lighter load and hence the redistribution is smaller. In accordance with Equation (10), if for a given beam the ultimate load decreases, the percentage of redistribution reduces too. Therefore, this is the main reason for which the redistribution drops when the degree of connection decreases.

The drop of the allowable redistribution when the degree of connection is changed from 1 to 0.75 is slighter than when it is reduced from 0.75 to 0.5; indeed, the last change leads to a sharp fall of the percentage of redistribution. The following graph (Figure 5.20) was obtained in order to understand this phenomenon. It shows the load slip curves and the state of the spring of one propped cantilever that connects the 51st and the 92nd nodes under the ultimate load due to rotation compatibility. This spring was specifically chosen because in this position is where maximum slips takes place, and hence, it represents the behaviour of the most stressed studs. Since the load-slip relationship for the studs is nonlinear as stated in section 2.1.3, and the idealization of this relationship is trilinear with different slope at each interval, the slip increase is not proportional to the drop of shear connection. Therefore, as the shear force under which the studs are working increases, their slip increases in a quicker way because stiffness reduces. As an example, the studs working in a system with a degree of connection of 0.75 experiences, for this beam, an increase in the ultimate slip of 0.75mm regarding the slip of the ones that works under full connection conditions. On the other hand,

the ones working in a 0.5 degree of connection system experiences an increase in the slip of 1.55mm regarding the slip of the ones that work under 0.75 degree of connection system. Consequently, if the slips increase in a quicker way with the drop of the degree of shear connection, the ultimate load will decrease in a quicker way, and then the allowable percentage of redistribution will drop more quickly, too.

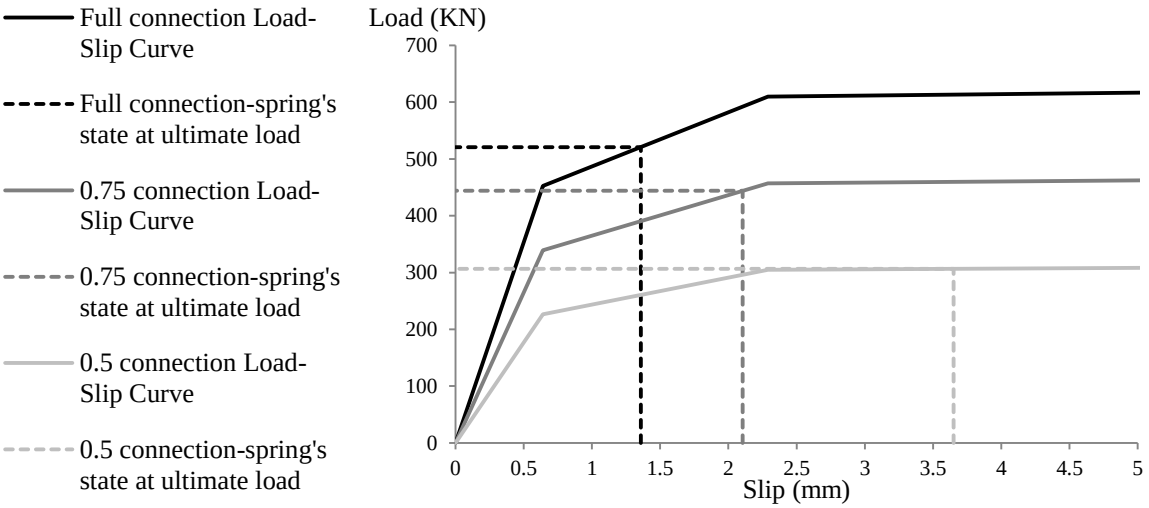

Figure 5.20: Load-Slip curves and ultimate states for the spring of the 10th node of the propped cantilever model for different grades of shear connection.

Finally, for those cases where there is not full connection, the behaviour of the component materials (concrete slab and structural steel) is uncoupled in a certain degree. This fact is explained by the presence of a neutral axis in both the concrete slab and the steel profile. The consequence of decreasing the degree of connection is that at hogging moment regions the capacity of reinforcing steel bars to transmit the tensile force to the structural steel is diminished. Therefore, the neutral axis tends to remain in a lower position towards the bottom flange. However, it will never be under the center of gravity of the I-section, since this position would be the one that belongs to a composite beam without shear connection system. The portion of the web under compression is smaller when the neutral axis is in a lower position. Consequently, the local buckling in the lowest fiber of the web becomes a less restrictive condition for the rotation capacity.

Table 5.1: Percentages of each type of rupture for Class-1 cross sections. Rotation compatibility.

Type of beam	Degree of connection	Flange	Web	Reinforcement
Propped	η=1	61.35	35.86	2.79
	η=0.75	71.13	28.87	0
	η=0.5	80.43	19.57	0
Fixed	η=1	52.76	45.53	1.7
	η=0.75	54.87	45.13	0
	η=0.5	70.73	29.21	0

Table 5.2: Percentages of each type of rupture for Class-2 cross sections. Rotation compatibility.

Type of beam	Degree of connection	Flange	Web	Reinforcement
Propped	η=1	0	100	0
	η=0.75	2.88	97.12	0
	η=0.5	43.6	56.4	0
Fixed	η=1	0	100	0
	η=0.75	0.41	99.57	0
	η=0.5	27.52	72.48	0

This is in accordance with the results summarized in Tables 2 and 3. For the web, the local buckling coefficient, K_σ, keeps changing towards less restrictive values when the neutral axis moves downwards. On the other hand, Kσ remains constant for the bottom flange since it is considered that the stress distribution remains uniform along the whole flange's width. Therefore, while the critical strain for local buckling at the flange remains constant when decreasing the degree of connection, the critical strain for local buckling at the web increases. Consequently, there are beams that, when they were designed with full interaction, failed due to local buckling at web, but when the degree of connection was decreased, the mode of failure changed to local buckling at the bottom flange. Therefore, as shown in Tables 2 and 3, for both Class-1 and Class-2 cross sections, and for both propped cantilevers and fixed end beams, there is a trend to increase the number of failures due to local buckling at bottom flange when the degree of shear connection is decreased.

5.6 Results of the parametric study.

As mentioned in Section 4, a parametric study with different non-dimensional parameters showed in Figure 4.2 was carried out. Interesting results were obtained from the study of the variation of the allowable redistribution against the reinforcement and steel area ratio and the concrete-steel ratio. Figures 5.21 and 5.22 show how the percentage of redistribution changes with these parameters for the case of beams of Class-1 with full shear connection. In the case of the Figure 5.21, it can be observed how the allowable redistribution tends to decrease when the reinforcement area increases regarding the steel profile area. This occurs due to the fact that an increase on the reinforcement area induces an increase of the neutral axis within the web, whose behaviour in the face of local buckling becomes weaker. Therefore, the beam tends to fail due to local buckling under lighter loads and hence the redistribution drops. On the other hand, Figure 5.22 shows that the redistribution tends to increase when the concrete-steel depth ratio increases. Therefore, for two beams that have exactly the same steel profile, with the same quantity of reinforcement, but with different concrete slab depth, the one that has a deeper concrete flange tends to have both steels less stressed at hogging moment regions with each increment of loading. Consequently, the loading capacity increases, and so does the redistribution.

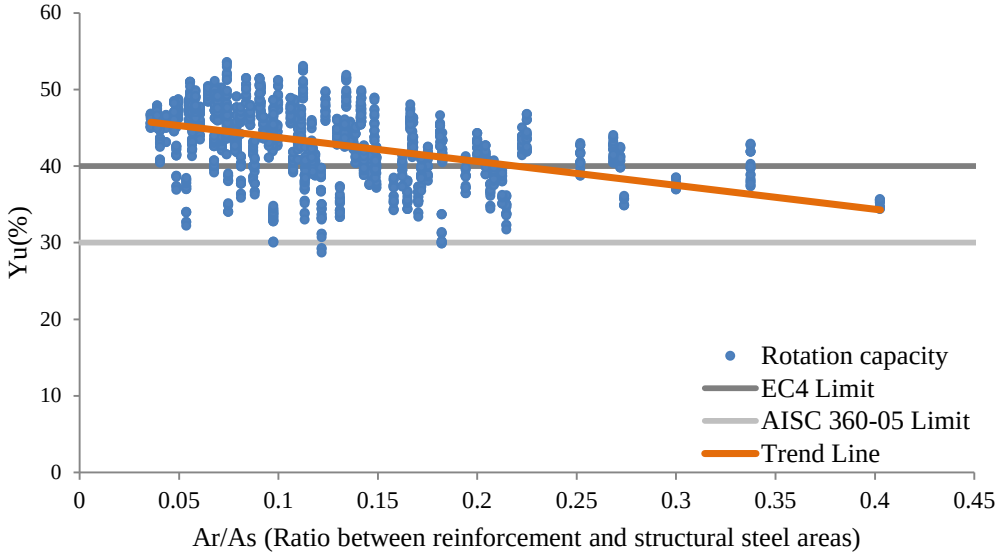

Figure 5.21: Permissible moment redistribution at ULS versus the reinforcement and steel area ratio for propped cantilevers.

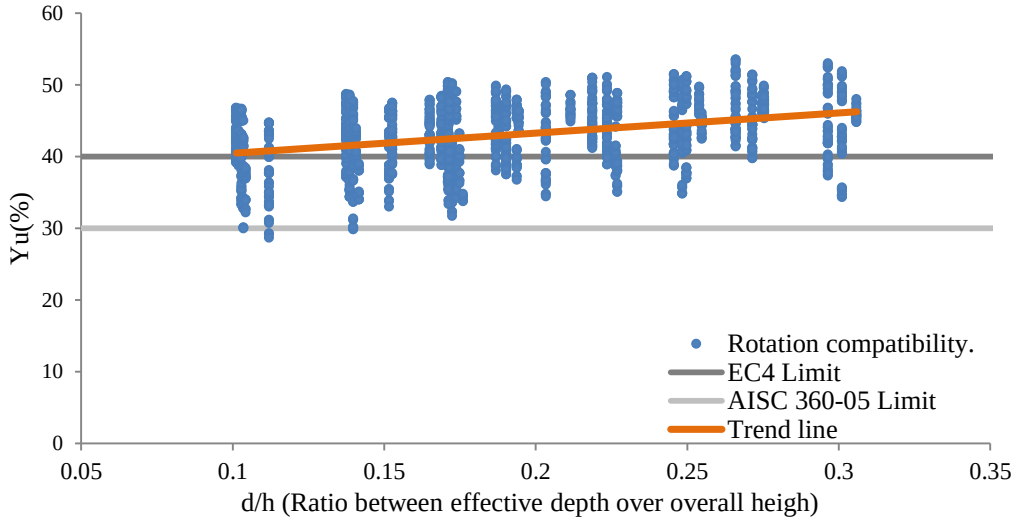

Figure 5.22: Permissible moment redistribution at ULS versus the concrete-steel depth ratio for propped cantilevers.

It must be pointed out that there is a noticeable deviation from the most of the points regarding the trend lines in the previous graphs. This is due to the fact of considering different values for a great deal of parameters such us mechanical properties, different steel profiles, different slab widths and depths, etc. Therefore, having higher redistribution in a beam that has a concrete-steel depth ratio equal to 0.1 than another one that has it equal to 0.3 can be a consequence of the variation of other parameters. The intention of this section was to study how the parameters shown affect to the redistribution when they are the unique parameter modified. It must be also mentioned that these trends are fulfilled for all the cases presented in Sections 5.1 and 5.2, since the numerical results demonstrate it.

5.7 Criteria of local buckling limits.

The limit for local buckling proposed by Kemp and Nethercot (2001) were also implemented to calculate the ultimate load for full connection cases. This research suggested that the critical compressive strain ε_{fb} in the bottom flange of the steel profile was determined by the following expression:

$$\varepsilon_{fb} = 1.33\left(\frac{t_f}{b_f}\right)^2 + 6.6\left(\frac{t_f}{L_p}\right)^2 \quad (16)$$

where t_f and b_f is the thickness and the breadth of the compression flange and L_p is the yielding length of the flange, which was assumed equal to 1.7 times the depth of the steel member (Kemp and Nethercot, 2001).

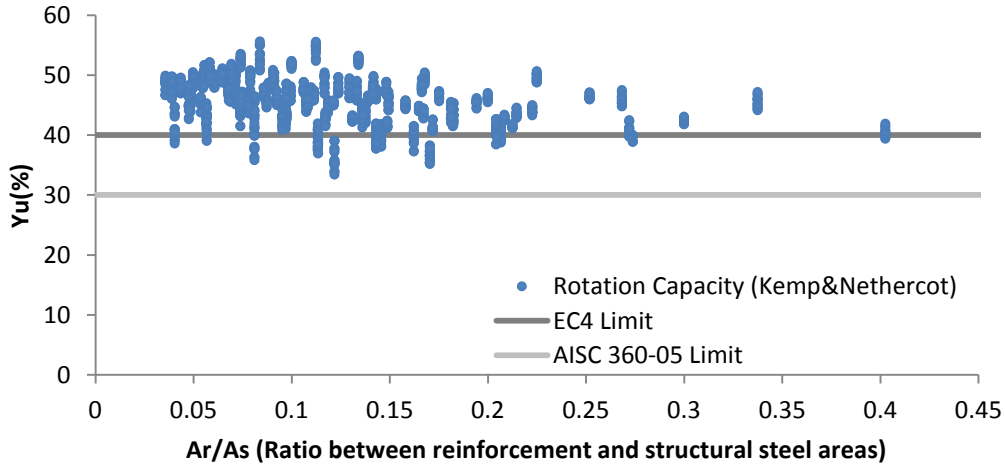

Figure 5.23: Permissible moment redistribution at ULS versus the reinforcement ratio for propped cantilevers. Class-1

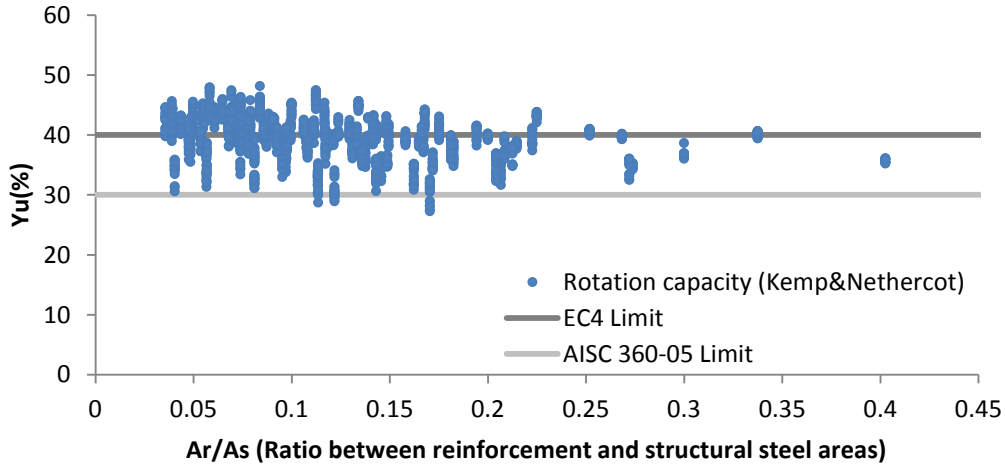

Figure 5.24: Permissible moment redistribution at ULS versus the reinforcement ratio for fixed end beams. Class-1.

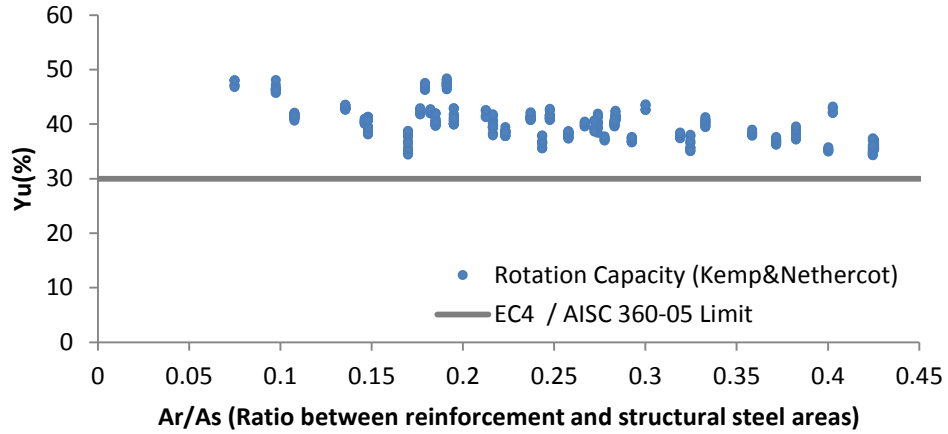

Figure 2.25: Permissible moment redistribution at ULS versus the reinforcement ratio for propped cantilevers. Class-2.

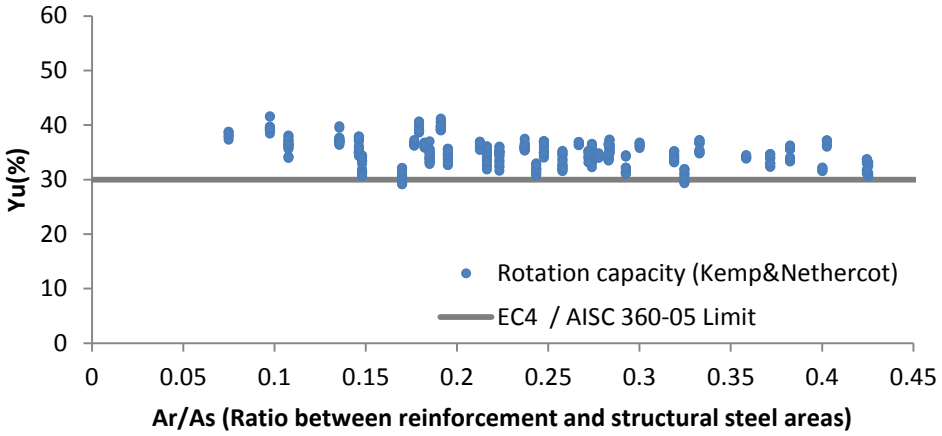

Figure 5.26: Permissible moment redistribution at ULS versus the reinforcement ratio for fixed end beams. Class-2.

The results, obtained using this criterion, are shown in the graphs within this section (Figures 5.23, 5.24, 5.25 and 5.26). It can be observed that now, the redistribution fulfills in a better way the limits stated by the American code (AISC 360-05, AISC 2005). This occurs because the criterion used to calculate the critical compressive strain in these cases is less restrictive than the one suggested by (Gardner et al, 2013). In Equation (3) is assumed a maximum allowable strain of $15\varepsilon_y$. It corresponds to the minimum ductility requirements stated by Eurocode 3 (CEN 2005) for structural steel.

As it is shown in Figure 5.27, for the range of beams that have been modeled in the present research, this limitation turns out to be the most restrictive condition to the allowable compressive strain at bottom flange. Therefore, since the criterion set out by Kemp and Nethercot (2001) does not consider this limitation, the strain limits are higher. Therefore, since the critical compressive strain is higher in accordance with this criterion, the rotation capacity is considered to be higher, and then the redistribution increases.

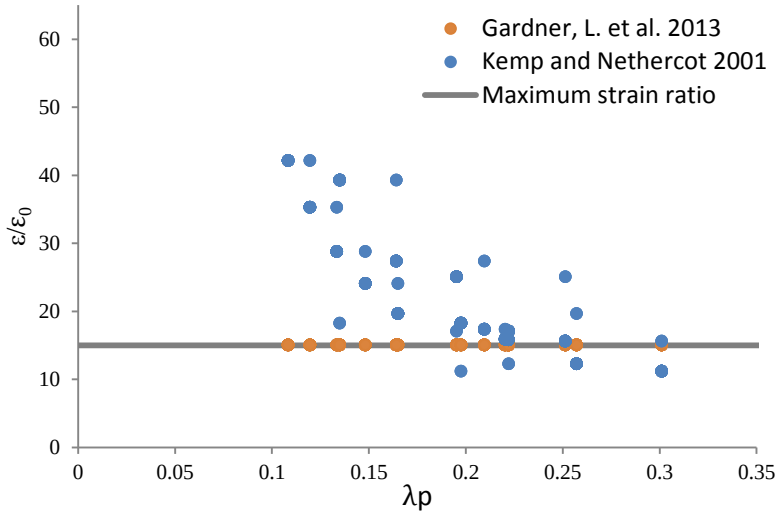

Figure 5.27: Limiting-yield strain ratio versus plate slenderness.

5.8 Suggestion of a redistribution domain.

With the results obtained within the sections 5.1 and 5.2, a domain for moment redistribution can be suggested for the cases when the continuous beam is under uniform distributed load with low ductility reinforcement in the concrete slab. As it has already been mentioned, this must be taken just as a conservative suggestion due to the fact that the results have been obtained using strict local buckling strain limits.

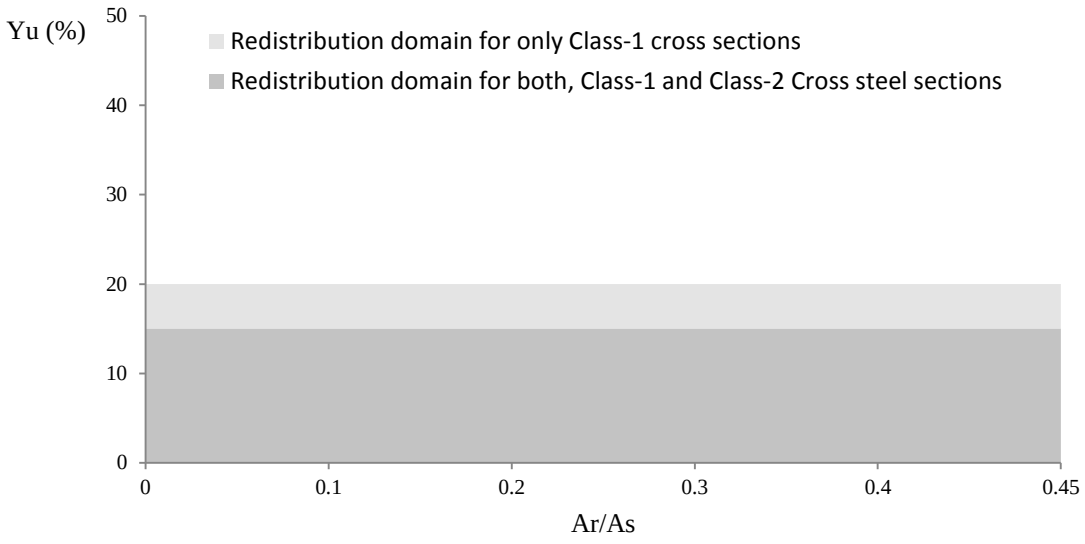

Figure 5.28: Suggested permissible moment redistribution domains for Class-1 and Class-2 sections at Ultimate Limit State

Figure 5.28 shows the suggested domains of permissible moment redistribution in the most possible generic way. It means that there are cases such as the ones of propped cantilevers of Class-2 cross steel sections for which the permissible moment redistribution could be a 20%

of the elastic bending moment at the fixed support, regardless of the shear connection degree. However, since the codes do not distinguish between propped cantilevers or fixed end beams, or in other words, they allow the same percentage of redistribution for both, external or internal spans of a continuous beams, it was found more appropriate suggesting the domains along the same line of action.

6. Conclusions.

A parametric study was carried out to investigate the influence of different parameters on the allowable moment redistribution at both, propped cantilevers and fixed end beams. Both the collapse due to mechanism formation and the collapse due to attainment of the rotation capacity (ULS) at long term period were taken into account for Class-1 and Class-2 cross steel sections (compact sections). Mainly, low ductility reinforcement (maximum elongation ε_{ru}=2.5%) has been assumed along the whole analysis. A finite element program purposely developed for nonlinear analysis for both short and long terms was used. In view of the results obtained from the study, the following conclusions can be made.

- In the case of full shear connection, the collapse of the beams occurred due to the attainment of the rotation capacity at fixed supports in all the cases for propped cantilevers. On the other hand, for fixed end beams, almost a 29% of the Class-1 beams collapsed due to the formation of a plastic mechanism. When the attainment of the rotation capacity was the cause of the collapse, the main type of failure was due to either local buckling at the bottom flange or at the lowest fiber of the web. However, there were few cases where the attainment of the maximum elongation at the reinforcement was the cause of failure.

- When the degree of connection is decreased, the number of collapses due to plastic mechanism formation reduces for Class-1 fixed end beams. Furthermore, no failures due to attainment of the maximum elongation at reinforcement were obtained. Finally, the fact of decreasing the degree of connection makes that the neutral axis remains in a lower position. Consequently, for some cases the local buckling at the bottom flange becomes a more restrictive condition than the local buckling at web. As a result, the percentage of failures due to local buckling at the bottom flange increases, whereas the percentage of failures due to local buckling at web decreases.

- When the ductility class of the reinforcement steel is increased up to normal ductility or high ductility steel, the local buckling at either bottom flange or web becomes the limiting phenomenon for the cases where the attainment of rotation capacity is the cause of failure.

- The results of the parametric study show that the values within the range of permissible moment redistribution tends to increase when the reinforcement and steel area ratio decreases.

- The investigation of the influence of the type of loading points out that the redistribution increases when the loading in a given beam is changed from point loading to third-point loading, and reaches its maximum when it is under uniform distributed load. Moreover, when the load is concentrated in a single point, the quick formation of a plastic mechanism prevents the beams from achieving similar percentages of redistribution to those achieved with the other types of loading.

- For Class-1 cross sections, the limit proposed by the Eurocode 4 (CEN 2004b) seems to be unconservative for some cases and under certain circumstances, since some modeled beams allow less redistribution than 40% of the elastic bending moment at the fixed support. On the other hand, the limit proposed by AISC 360-05 seems to be on the safe side for propped cantilevers when the degree of connection is between 0.75

and 1. However, for fixed end beams it does not seem to be very conservative. When the degree of shear connection decreases up to 0.5, most of the beams modeled have less allowable moment redistribution than 30%.

- For Class-2 cross sections, the limit proposed by the codes taken into account seems to be in most of the cases unconservative.

- The criterion used to evaluate the critical compressive strain, in either the bottom flange or the web, seems to be stricter than others used in previous research. As a result, the allowable moment redistribution tends to decrease, being in a more conservative range.

In conclusion, the results of the study show that, for the mechanical properties and geometric features considered, with low ductility steel, the permissible moment redistribution at Ultimate Limit State should be as maximum a 20% of the elastic bending moment for Class-1 cross sections, and a 15% of the elastic bending moment for Class-2 sections. However, it must be emphasised that these limits might be a conservative suggestion, since strict criteria have been assumed for local buckling. Moreover, further research such as experimental one is suggested in order to validate these results, which seem to be quite conservative.

7. References.

Abdollahi, A. (1996) Numerical strategies in the application of the FEM to RC structures - I. Computers and Structures. 58 (6), 1171-1182.

AISC. (2005). Specification for structural steel buildings. AISC 360-05, Chicago, Il1.

Comite Euro-International du Beton (CEB). (1993). CEB-FIP model code 90. CEB Bull. No. 213/214, London, Thomas Telford Publishing.

Corus Construction & Industrial. (2007) Advanced sections. CE marked structural sections. Scunthorpe, Corus Construction Services & Development.

European Committee for Standardization (CEN). (2002) Eurocode 0-Basis of structural design. EN-1990, Bruxelles, Belgium.

European Committee for Standardization (CEN). (2004.a) Eurocode 2-Design of concrete structures. Part 1-1: General rules and rules for buildings. EN-1992-1-1, Bruxelles, Belgium.

European Committee for Standardization (CEN). (2004.b) Eurocode 4-Design of composite steel and concrete structures. Part 1-1: General rules and rules for buildings. ENV-1994-1-1, Bruxelles, Belgium.

European Committee for Standardization (CEN). (2005) Eurocode 3-Design of steel structures. Part 1-1: General rules and rules for buildings. EN-1993-1-1, Bruxelles, Belgium.

European Committee for Standardization (CEN). (2006) Eurocode 3-Design of steel structures. Part 1-5: Plated Structural Elements. EN-1993-1-5, Bruxelles, Belgium.

Fragiacomo, M., Amadio, C. & Macorini, L. (2004) Finite-element model for collapse and long-term analysis of steel-concrete composite beams. Journal of Structural Engineering. 130 (3), 489-497.

Gardner, L. (2008) The continuous strength method. Proceedings of the Institution of Civil Engineers: Structures and Buildings. 161 (3), 127-133.

Gardner, L., Macorini, L. and Kucukler, M. (2013). The continuous strength method for steel and composite design. Institution of Civ. Engrs. Volume 166 Issue SB1 (Under publication)

Gattesco, N. and Cohn, M. Z. (1989) Computer simulated tests on moment redistribution. Part I: ULS consideration. Studi e Ricerche, F.lli Pesenti. n.11, Politecnico di Milano, Italy, 269-299

Gattesco, N., Macorini, L. and Fragiacomo, M. (2010) Moment redistribution in continuous steel-concrete composite beams with compact cross section. Journal of Structural Engineering. 136 (2), 193-202.

Hendy C. R., Johnson, R. P. (2006) Designers' guide to EN 1994-1-1 Eurocode 4: Design of composite steel and concrete structures. Part 2: General rules and rules for bridges. London, Thomas Telford Publishing.

Izzuddin B.A. (1991), Nonlinear dynamic analysis of framed structures. PhD. Thesis, Imperial College.

Johnson, R. P. and May, I. M. (1975) Partial-interaction design of composite beams. Struct. Eng., 53(8), 305-311

Johnson, R. P. & Molenstra, N. (1991) Partial shear connection in composite beams for buildings. Proceedings - Institution of Civil Engineers. Part 2. Research and Theory. 91, 679-704.

Johnson, R. P. (2004) Composite structures of steel and concrete. Beams, slabs, columns, and frames for buildings. 3rd ed.Oxford Blackwell Publishing.

Johnson, R. P., Anderson D. (2004) Designers' guide to EN 1994-1-1 Eurocode 4: Design of composite steel and concrete structures. Part I.I: General rules and rules for buildings. London, Thomas Telford Publishing.

Kemp, A. R. & Nethercot, D. A. (2001) Required and available rotations in continuous composite beams with semi-rigid connections. Journal of Constructional Steel Research. 57 (4), 375-400.

Mander, J. B., Priestley, M. J. N. and Park, R. (1988) Theoretical stress-strain model for confined concrete. Journal of Structural Engineering New York, N. Y. 114 (8), 1804-1826.

Ollgaard, J. G., Slutter, R. G. & Fisher, J. W. (1971) Shear strength of stud connectors in lightweight and normalweight concrete. 8 (2), 55-64.

Sebastian W. M., McConnel R.E. (2000). Nonlinear FE analysis of steel-concrete composite structures. Journal of Structural Engineering. Vol. 126, No. 6, June, 2000.

Teraskiewicz, J. S. (1967). Static and fatigue behaviour of simply supported and continuous composite beams of steel and concrete. PhD thesis, University of London, England.

Titoum, M., Tehami, M., Achour, B. (2009). Effects of partial shear connection on the behavior of semi-continuous composite beams. International Journal of Steel Structures. Vol. 9, No.4, 301-313.

Yam L. C. P., Champan, J.C. (1972). The inelastic behaviour of continuous composite beams of steel and concrete. Proc., Institution of Civ. Engrs., 2(53), December, 487-501.